Geochimica et Cosmochimica Acta 360 (2023) 192–206

Contents lists available at ScienceDirect

Geochimica et Cosmochimica Acta

journal homepage: www.elsevier.com/locate/gca

The effect of biogeochemical redox oscillations on arsenic release from legacy mine tailings

Yizhang Liu [a,b], Robert A. Root [a], Nate Abramson [c], Lijun Fan [a,d], Jing Sun [b], Chengshuai Liu [b], Jon Chorover [a,e,*]

[a] Department of Environmental Science, University of Arizona, 1177 E. 4th Street, Tucson, AZ 85721-0038, USA
[b] State Key Laboratory of Environmental Geochemistry, Institute of Geochemistry, Chinese Academy of Sciences, Guiyang 550081, China
[c] Department of Geosciences, University of Arizona, 1040 E. 4th Street, Tucson, AZ 85721-0077, USA
[d] College of Environment, Zhejiang University of Technology, Hangzhou 310014, China
[e] Arizona Laboratory for Emerging Contaminants, University of Arizona, 1040 E. 4th Street, Tucson, AZ 85721-0077, USA

ARTICLE INFO

Associate editor: Georges Calas

Keywords:
Redox
Phytostabilization
Bioreactor
Arsenic release
Iron speciation

ABSTRACT

Exposed and un-remediated metal(loid)-bearing mine tailings are susceptible to wind and water erosion that disperses toxic elements into the surrounding environment. Compost-assisted phytostabilization has been successfully applied to legacy tailings as an inexpensive, eco-friendly, and sustainable landscape rehabilitation that provides vegetative cover and subsurface scaffolding to inhibit offsite transport of contaminant laden particles. The possibility of augmented metal(loid) mobility from subsurface redox reactions driven by irrigation and organic amendments is known and arsenic (As) is of particular concern because of its high affinity for adsorption to reducible ferric (oxyhydr)oxide surface sites. However, the biogeochemical transformation of As in mine tailings during multiple redox oscillations has not yet been addressed. In the present study, a redox-stat reactor was used to control oscillations between 7 d oxic and 7 d anoxic half-cycles over a three-month period in mine tailings with and without amendment of compost-derived organic matter (OM) solution. Aqueous and solid phase analyses during and after redox oscillations by mass spectrometry and synchrotron X-ray absorption spectroscopy revealed that soluble OM addition stimulated pyrite oxidation, which resulted in accelerated acidification and increased aqueous sulfate activity. Soluble OM in the reactor solution significantly increased mobilization of As under anoxic half-cycles primarily through reductive dissolution of ferrihydrite. Microbially-mediated As reduction was also observed in compost treatments, which increased partitioning to the aqueous phase due to the lower affinity of As(III) for complexation on ferric surface sites, e.g. ferrihydrite. Oxic half-cycles showed As repartitioned to the solid phase concurrent with precipitation of ferrihydrite and jarosite. Multiple redox oscillations increased the crystallinity of Fe minerals in the Treatment reactors with compost solution due to the reductive dissolution of ferrihydrite and precipitation of jarosite. The release of As from tailings gradually decreased after repeated redox oscillations. The high sulfate, ferrous iron, and hydronium activity promoted the precipitation of jarosite, which sequestered arsenic. Our results indicated that redox oscillations under compost-assisted phytostabilization can promote As release that diminishes over time, which should inform remediation assessment and environmental risk assessment of mine site compost-assisted phytostabilization.

1. Introduction

Mining activities generate approximately 5 billion tons of tailing wastes per year, estimated to equal the amount of global mass movement of Earth material by geological processes (Hudson-Edwards et al., 2011; Lu and Wang, 2012). Sulfidic mine waste from polymetallic ore beneficiation can be enriched in toxic elements that present health risks to the surrounding environment and population (Root et al., 2015). Mine wastes generally present low organic matter and nutrient content, weak water holding and penetrating capacity, and low abundance of heterotrophic bacteria, and sulfidic tailings, in particular, also exhibit acidic pH and high contents of toxic chalcophile metal(loid)s such as Pb,

* Corresponding author at: Department of Environmental Science, University of Arizona, 1177 E. 4th Street, Tucson, AZ 85721-0038, USA.
E-mail addresses: liuyizhang@mail.gyig.ac.cn (Y. Liu), rroot@arizona.edu (R.A. Root), nabramso@arizona.edu (N. Abramson), fanlijun@zjut.edu.cn (L. Fan), sunjing@mail.gyig.ac.cn (J. Sun), liuchengshuai@vip.gyig.ac.cn (C. Liu), chorover@arizona.edu (J. Chorover).

https://doi.org/10.1016/j.gca.2023.09.012
Received 2 February 2023; Accepted 13 September 2023
Available online 16 September 2023

Zn, As and Cu (Solís-Dominguez et al., 2012; Jamieson et al., 2015; Lindsay et al., 2015; Hammond et al., 2020). These biogeochemical conditions inhibit plant establishment and vegetative cover thereby exposing the tailings to wind and water erosion that can transport contaminants as fugitive dust or colloidal and/or dissolved metal(loid)s (Stovern et al., 2014; Abraham and Susan, 2017; Gil-Loaiza et al., 2018; Root and Chorover, 2022). Hence, remediation strategies are needed to reduce the offsite migration of toxic metal(loid)s. Phytostabilization is an eco-friendly technique that uses plants and amendments (such as microbes, organic residues, and irrigation water) to establish a vegetative cover that inhibits the offsite transport of toxic elements (Mendez and Maier, 2008; Bolan et al., 2011; Kohler et al., 2015). Compost is commonly used to assist phytostabilization in nutrient-poor, inhospitable contaminated environments (Kohler et al., 2015; Gil-Loaiza et al., 2016). Compost amendments act as a nutrient source, improve water and nutrient holding capacity, increase microbial activity, and buffer acidification (Fagnano et al., 2011; Valentín-Vargas et al., 2014; Nelson et al., 2015; Visconti et al., 2020).

Compost- and irrigation-assisted phytostabilization was successfully applied to contain off-site dust emissions of As and Pb contaminated tailings at the Iron King mine Humboldt Smelter Superfund Site, in central AZ, USA (Fig. S1) (Gil-Loaiza et al., 2016; Hammond et al., 2020). However, redox changes may drive biogeochemical reactions such as dissolution, adsorption/desorption, complexation and redox reactions at micro-interfaces in tailings systems (Huang et al., 2016; Bozeman, 2018; Visconti et al., 2020; Hammond et al., 2020). Among these, the impact on the mobility of As is of particular concern since As is a redox-sensitive toxic metalloid that commonly concentrates in sulfide mineral ores (O'Day, 2006; Lengke et al., 2009; Root et al., 2015). During surficial weathering of sulfide tailings, As speciation may be transformed from sulfide-bound to bonded association with Fe minerals such as scorodite, schwertmannite, ferrihydrite and jarosite through sorption, coprecipitation and incorporation pathways (Root et al., 2015; Hammond et al., 2020). Therefore, the mobility and fate of As in weathered tailings is highly associated with Fe speciation and mineralogy. Additionally, As has a high affinity for organic amendments such as compost and OM coated grains. Conversely, organic compounds and (oxy)anions released from compost (e.g., SO_4^{2-}, PO_4^{3-}) may compete for surface sites on Fe minerals with As and increase As mobility (Bauer and Blodau, 2006; Bozeman, 2018). For instance, soluble organic matter is known to significantly enhance the mobilization of As, with precise effects varying with concentration and pH (Wang and Mulligan, 2009a,b). Phosphate has also been shown to influence As mobility by competing for sorption sites (Goh and Lim, 2005). Dissolved organic carbon is widely regarded as a key factor responsible for the microbial reductive dissolution of As-bearing Fe (hydr)oxide minerals in anoxic environments (Islam et al., 2004; Mladenov et al., 2015). Therefore, compost addition in tailings was hypothesized to promote As mobility, which has important implications for the success of phytostabilization.

The effects of compost addition on As mobility and speciation have been reported in previous studies on experimental and field samples (Hartley et al., 2010; Beesley et al., 2014; Bozeman, 2018; Hammond et al., 2020). However, geochemical changes resulting from repeated redox oscillations, a phenomenon that exists at many field sites, including those impacted by irrigation, have not been addressed. Redox conditions at the bulk- and micro-scales may fluctuate due to periodic flooding, irrigation and fluctuation of groundwater. This oscillation has been proven to influence the crystallinity of Fe oxides, and the transformation of Fe oxides is likely to be influenced by the initial Fe mineral composition and leaching rate (Thompson et al., 2006; Winkler et al., 2018). Iron oxide crystallinity decreased in soils rich in crystalline Fe oxides subject to constrained leaching but crystallinity increased in soils rich in short-range ordered (SRO) Fe oxides subject to well-drained conditions (Winkler et al., 2018). These cumulative effects are expected to influence the mobility of As, which is tightly coupled to the geochemical transformations of Fe (Fendorf and Kocar, 2009; Root et al., 2009). In redox oscillation experiments, Parsons et al. (2013) found that As mobility in calcareous soil was decreased by up to 45% during anoxic half-cycles, and Fe dynamics were regarded as the key driver of such effects. Similar experimental studies on sediments showed that Fe is a vital control on As mobilization/immobilization during redox oscillations (Phan et al., 2018; 2019). However, the effects of redox oscillations in tailings materials are less well known, as sulfide tailings are circumscribed by distinct geochemical characteristics (e.g., extremely high Fe and As, low pH and nutrients, simple and limited microbial communities). Hence, the biogeochemical processes and effects in metalliferous tailings subjected to redox oscillations may differ as well, particularly in respect to the fate of As, with important implications for irrigated phytostabilization.

At the Iron King Mine and Humboldt Smelter Superfund Site (IKMHSS), in Dewey-Humboldt, Arizona, approximately four million cubic meters of sulfide tailings were contained in 62 ha and piled to a maximum thickness of approximately 30 m. These tailings are characterized by high concentrations of Fe (>10%), S (~10%) and toxic metal (loid)s (As, Pb and Zn > 2000 mg kg^{-1}), extremely low pH (~2.5) and low total carbon and nitrogen (around detection limits) (Hayes et al., 2014; Root et al., 2015; Gil-Loaiza et al., 2016). Approximately 30% of the near surface Fe exists in ferrihydrite, which hosts the majority of As in the form of As(V) (Root et al., 2015). Compost assisted phytostabilization was conducted on site to reduce wind and water erosion and to control risks to nearby communities and ecosystems, not only to buffer the pH but also introduce beneficial nutrients and microbes to promote plant growth (Nelson et al., 2015; Gil-Loaiza et al., 2016, 2018). However, compost may also have adverse effects on the mobility of As. Batch experiments showed that a "compost tea" treatment released approximately 70% more As to the solution than the control group, and column experiments showed that anion competition and ligand exchange contribute to the mobilization of As (Bozeman, 2018). Field work showed that downward translocation of As was both observed in compost amendment and non-amended control tailings, both were irrigated (Hammond et al., 2020). These data may suggest that released As was immobilized under oxic conditions. Therefore, associated biogeochemical transformation of Fe and As in tailings is expected during redox oscillations with compost amendment. In the present study, we hypothesized that introducing labile soluble organic carbon from compost would facilitate reductive dissolution of Fe minerals and thereby mobilize As under anoxic environment, but that As would repartition to the solid phase during oxic environment. Furthermore, we postulated that a change in crystalline character of Fe oxides during redox oscillations would impact the sequestration of As over multiple redox cycles. To test our hypotheses, a redox-stat reactor system was designed for tailings reacted with compost solution or an equivalent ionic strength electrolyte for 7 redox cycles, with each cycle including 7 d anoxic + 7 d oxic (Fig. S2). The aqueous chemistry, mineralogy and solid phase speciation of As and Fe during and after oscillations was analyzed by conjunctive use of wet chemical and spectroscopic methods.

2. Materials and methods

2.1. Experimental samples

Mine tailings used in this study were collected from the surface layer (0–25 cm) of IKMHSS, a well-characterized sulfide-ore tailings U.S. Environmental Protection Agency (USEPA) listed Superfund Site for which the geological and geochemical background has been described in detail elsewhere (Hayes et al., 2014; Root et al., 2015; Hammond et al., 2020). Tailings were homogenized, screened to 2 mm and then ground to <425 μm. Solid compost made from organic plant and manure waste (Tank's Green Stuff ™, 100% Organic Compost, Tucson, AZ) was the same as that used at the field site for phytostabilization, which was crushed and sieved to <425 μm. Total concentrations of elements in solid samples were measured by inductively coupled plasma mass

spectrometry (ICP–MS, Agilent 7700x, Santa Clara CA) following microwave assisted acid digestion in the Arizona Laboratory for Emerging Contaminants (ALEC). Total carbon (TC), nitrogen (TN) and sulfur (TS) of the solids were measured by a CHNSO gas chromatograph analyzer (Costech ECS 4010, Valencia, CA) in ALEC. The crushed compost was mixed with type-I deionized water (18.2 MΩ-cm) at a solid to solution ratio of 1:10 (m/m) in the dark to create a compost solution or "compost tea" (Bozeman, 2018). The mixture was allowed to settle for 30 min and then filtered through a 46 μm sieve, followed by a 1 μm filter bag (Welded Industrial Filter Sock Bags) and used fresh. Geochemical conditions at the onset of the experiment (time zero, "t_0") were analyzed in samples prepared from tailings mixed with electrolyte or compost solution with solid to solution ratio as reactors. These samples were assumed to provide unreacted t_0 information and were used for comparative analysis subsequent characterizations, including selective sequential extraction, XRD, and XAS techniques.

2.2. Redox reactor setup

A bench-scale redox-stat reactor system with a working volume of 1 L per reactor was designed and assembled based on previous studies (Thompson et al., 2006; Parsons et al., 2013). Briefly, the redox conditions were controlled by switching between nitrogen and air sparging at a flow of 40 mL min^{-1}, monitored with a flow meter (Fig. S2). Electrochemical monitoring Eh and pH electrodes (Mettler Toledo) were connected through threaded ports on the lid of the reactor, and data were recorded every 10 min to a data logger (Campbell CR1000, USA). The gas outlet port was connected with a one-way gas test valve to exclude influences from the ambient environment. Magnetic stirring (VWR) was used to mix the suspensions. Four reactors were run in tandem, with duplicates for the Control (tailing + electrolyte) and Treatment (tailing + compost solution) experiments. All components were acid washed and rinsed with 18.2 MΩ-cm deionized water. Aqueous aliquots were collected as a function of time by syringe. To compare the data from the data logger and meter, Eh and pH was also recorded at every sampling time.

2.3. Experimental procedure

Fifty grams of ground tailings (<425 μm) were weighed into each reactor, 1000 g of compost solution were added to the treatment group (Treatment C, Treatment D), and 1000 g of electrolyte solution (10 mM NaCl + 25 mM KCl) with similar ionic strength to the compost solution were used in the control group (Control A, Control B). This 1:20 tailing to solution mass ratio was selected to facilitate a well-mixed suspension representative of the reactivity occurring in tailing pore fluids. To exclude the influence of electrolyte on mineral saturation state, NaCl was used to compensate for the ionic strength of other ions (except K^+). The initial pH of the compost solution and electrolyte was adjusted to 4.5 before mixing. Then, the suspension pH was again adjusted to 4.5 after mixing and equilibration for 24 h through the addition of HCl and NaOH, change in volume was <1%. A total of 7 full redox cycles (14 d for each full cycle, including a 7-day anoxic half-cycle and a 7-day oxic half-cycle) were conducted for 98 days at room temperature and the temperature in solution was maintained at 29.5 ± 2.0 °C. To test the influence of the labile carbon source, at the beginning of the 6th and 7th anoxic half-cycles, 0.25 g glucose was added to the reactors, and the pH was adjusted to 4.5 with NaOH.

Samples were collected at the end of day 1, 4 and 7 of each half-cycle, 6 mL samples were collected at day 1 and 4, 8 mL samples were collected at day 7. Samples were separated into 3 aliquots, one mL for archival purposes, 1 mL centrifuged at 22,000 relative centrifugal force (RCF) for 45 min to separate suspension, and the solids were then extracted in 0.5 M HCl for 2 h at room temperature, centrifuged at 22,000 RCF for 6 min, supernatant solution carefully aspirated by pipette for Fe(II) and total Fe measurement to quantify adsorbed Fe^{2+} and soluble short-range-ordered (SRO) Fe oxides (Thompson et al., 2006). The remaining samples were centrifuged at 3200 RCF for 15 min and filtered to 0.45 μm with a GHP Acrodisc syringe filter. Samples from the anoxic half-cycle were transferred into an anoxic glove box (N_2:H_2, 97:3) for processing. Solutions were used for the wet chemistry measurements, and solids were frozen at −125 °C and then freeze-dried prior to sequential extraction, XAS and XRD.

2.4. Aqueous chemistry measurement

Aqueous chemistry measurements were conducted in ALEC. Cations and total As were measured by ICP–MS as mentioned above, and anions were analyzed by ion chromatography (Dionex ICS-1000, Sunnyvale, CA). Arsenic speciation was preserved by the addition of 0.25 M EDTA (Bednar et al., 2002) prior to measurement by HPLC-ICP–MS. Ferrous iron was measured by the ferrozine method (Stookey, 1970) with a UV–vis spectrophotometer (Shimadzu UV-301 PC), and Fe(III) was calculated by subtracting Fe(II) from total Fe measured by ICP–MS. Dissolved organic carbon (DOC) measurements were achieved by a Shimadzu 5000A TOC analyzer. The dissolved organic matter functional group chemistry was analyzed in the compost leachate by FTIR (Nicolet 6700 spectrometer, Madison, WI), details in the SI.

2.5. Chemical extraction

Ferrous Fe bound to the solid surface and incorporated into SRO Fe oxides in the pellets following centrifugation were extracted in 0.5 M HCl for 2 h at room temperature on an end-over-end rotator (Thompson et al., 2006). Based on previous extraction results (Hayes et al., 2014; Root et al., 2015), a simplified three-step sequential extraction procedure was applied to freeze-dried solid samples on day 7 of the 1st, 3rd, 5th and 7th half cycles and the time 0 samples. Briefly, (1) sodium phosphate targeting adsorbed As (1 M NaH_2PO_4, pH = 5.0, 24 h, 25 °C), (2) acid ammonium oxalate (AAO) targeting reducible poorly crystalline Fe oxides (0.2 M, pH = 3, dark, 2 h, 25 °C) and, (3) citrate-bicarbonate-dithionite (CBD) targeting reducible crystalline Fe oxides (pH = 7, dark, 2 h, 80 °C) were applied at solid to solution ration of 1:100. These three steps accounted for most of the Fe and As pools (Hayes et al., 2014; Root et al., 2015).

2.6. X-ray techniques

Iron and arsenic K-edge X-ray absorption spectroscopy (XAS) spectra were collected on beamline 11-2 at the Stanford Synchrotron Radiation Lightsource (SSRL; Menlo Park, CA, USA) using methods detailed elsewhere (Hayes et al., 2014; Root et al., 2015). In brief, Fe and As XAS were collected with a double-crystal monochromator (Si [2 2 0] crystal, φ = 90) using a 100-element Ge array fluorescence detector under an LN_2-cooled sample cryostat to avoid beam damage and to minimize thermal disorder in the structure. Data processing was performed by SIXPACK (Webb, 2005) and Athena (Ravel and Newville, 2005) software packages. XRD data were collected at SSRL on beamline 11-3 and processed as described by Hayes et al. (2014).

2.7. Data expression

Aqueous phase speciation and mineral saturation indices were calculated using Geochemist's Workbench (GWB, v9). The Eh voltage value was calibrated relative to the standard hydrogen electrode (SHE). Variation in suspended solid concentrations and entrained solution was excluded by measuring the mass of dried solid and wet pellets from 0.5 M HCl extraction, the extraction concentration of elements was calculated based on dry mass and expressed as mmol per kilogram (mmol kg^{-1}). The chemical concentration in the solution was expressed in millimoles or micromoles per liter (mM or μM).

3. Results

3.1. Initial sample characterization

The original tailings were characterized by high concentrations of Fe, S and As, low C and N, and extremely low pH (Table 1). Principal minerals included quartz, jarosite, gypsum, and pyrite. The solid phase Fe concentrations extracted by AAO and CBD solutions were 647 and 737 mmol kg^{-1}, respectively. Hence, *ca.* 38% and 43% of total Fe were hosted in extracted fractions defined operationally as amorphous (AAO extracted) and crystalline (CBD extracted), respectively. Arsenic extracted by NaH_2PO_4, AAO and CBD amounted to 6.19, 24.9, and 2.81 mmol kg^{-1}, respectively, accounting for approximately 18%, 73%, and 8% of the total As. Solid compost presented much higher carbon (TC) and nitrogen (TN) but lower sulfur (TS) than tailings. Dominant cations in the extracted compost solution were K^+ and Na^+, whereas soluble Fe and As were low (Table 1). Approximately 3% of TC in compost was water soluble, consistent with previous results (Bozeman, 2018). FTIR identified broad absorption peaks centered at 3380 cm^{-1} from the O—H vibration of alcohols, phenols, and organic acids; smaller peaks at 2937–2852 cm^{-1} from the C—H stretching of aliphatic chains and alkanes; C═O vibrations form carboxyl and carboxylic acid (in pH adjusted DOM) at 1712–1639 cm^{-1}; fulvic acid and aliphatic chains at 1410 cm^{-1}; protein compounds at 1385 cm^{-1}; C—O stretching of polysaccharide at 1047 cm^{-1}, and sharp peaks in the unacidified DOM leachate at 669, 837,1385, and 2340 cm^{-1} from carbonate that are not present in the spectrum from the pH 4.5 compost DOM (Fig. S3). The pH of the influent compost solution was adjusted to 4.5 by HCl to diminish its buffer capacity in reactors and to obtain similar experimental conditions.

3.2. Aqueous Chemistry

3.2.1. Eh, pH and DOC in solution

Redox fluctuation was modulated by sparging with N_2 or ultra-high purity compressed air (Fig. S2). As expected, the oxidation potential (Eh) in solution gradually decreased during anoxic half-cycles and rapidly increased in oxic half-cycles (Fig. 1a). The Eh values in compost solution Treatments C and D were highly consistent, with a range of approximately 200–300 mV for the first 5 full cycles. Control A showed smaller Eh variation than Control B for the first three cycles, but these reactors later converged to similar Eh fluctuation amplitudes. The compost Treatment group (C and D) displayed a 200 mV higher Eh than the Control group (A and B) before the addition of glucose. The addition of glucose and re-adjustment of pH substantially lowered Eh in anoxic half-cycles. Generally, solution pH increased in the anoxic half-cycle and decreased in the oxic half-cycle (Fig. 1b). An exception was that the pH in control A did not significantly change in the first three cycles. The pH in the control set was very consistent, but the pH in the treatment set dropped to ca. 2.2 in the first two cycles.

The DOC in Treatments dropped from ~45 mM to ~20 mM after 1 d of reaction (Fig. 1c), with the bulk of the rapid 55% decrease in DOC likely resulting from adsorption to the tailings (with a smaller contribution from microbial degradation). The DOC decreased during oxic half-cycles and increased during anoxic half-cycles for the Treatment set. When 0.25 g glucose was added to reactors at the beginning of the 6th and 7th anoxic half-cycles (days 70 and 84), the increase of DOC after 24 h was approximately 12 mM for the Control set (A, B) and 7 mM for the Treatment set (C, D).

3.2.2. Concentration and aqueous speciation dynamics of S, Fe and As

Sulfate (SO_4^{2-}) in the four reactors ranged from 21.4 mM to 58.4 mM over the course of the experiment, and there were significant differences between the Control and Treatment groups (Fig. 1d). All reactors showed increases in sulfate concentration with time, but compost treatments showed much larger increases (Table S1). Whereas Controls showed no effect of redox half-cycles, compost treatments showed increases in sulfate during oxic half-cycles, followed by some decreases during the anoxic half-cycles, particularly in Treatment C. For the Controls, SO_4^{2-} fluctuated (21.4–36.9 mM) in the first two full cycles and then remained relatively constant for the rest of the experiment (28.2–34.9 mM), whereas in the OM Treatments, SO_4^{2-} increased from 26.5 ± 0.5 mM at the start to 48.5 ± 2.2 mM at the end, and the amplitude of redox fluctuation was as high as *ca.* 20 mM.

Total dissolved Fe (Fe^T) gradually increased in the anoxic half-cycles and dropped on the first day of the oxic half-cycles, except for the first cycle, where all treatments remained fairly constant (Fig. 1e). The influence of Fe^T from compost solution (~0.05 mM) was negligible considering that the concentration of Fe^T in these reactors >0.5 mM at the 1st day. Soluble Fe was quantifiable as both Fe^{2+} and Fe^{3+} in anoxic and oxic half-cycles (Fig. 2). The Treatment reactors showed higher [Fe^{2+}] at the end of each anoxic half-cycle than the Controls. In the oxic half-cycles, [Fe^{2+}] decreased rapidly, and [Fe^{3+}] in the Control reactors was close to non-detectable. Speciation of Fe modeled by GWB at measured dissolved ion activities showed that the dominant Fe species should be Fe^{2+} and $FeSO_{4(aq)}$ in reducing half-cycles, and Fe^{3+} and $FeSO_{4(aq)}^+$ during oxic half-cycles.

Arsenic was mobilized in anoxic half-cycles in the presence of compost, reaching up to 23.1 μM (approximately 1.58% of total As in solid) and 17.1 μM in Treatment C and D, respectively. The relatively high concentration of total As indicated that dissolved As in compost solution (0.60 μM) was insignificant in its contribution to the aqueous phase totals. In Controls, the highest [As] concentration encountered was 5.94 μM (Control B). Arsenic solubilized during anoxic half-cycles was re-sorbed during subsequent oxic half-cycles. As was the case for Fe, there was a one cycle lag before the release/retention pattern for As was observed to manifest. After the initial cycle, both As(III) and As(V) increased in anoxic half-cycles and decreased in oxic half-cycles (Fig. 2). Most of the As was mobilized as As(V), accounting for ≥60% in the Treatment reactors before the addition of glucose at 70 d. The presence

Table 1
Chemical composition of experimental samples.

Sample	Na^+	K^+	Ca^{2+}	Fe	As	TN	TC	TS	pH
	mmol kg^{-1}						g kg^{-1}		
Tailings	2.28	113	132	1709	31.7	BDL	1.3	51.7	2.78
Compost	63.6	90.9	90.8	92.3	0.038	10.3	171.3	4.1	7.45
	Na^+	K^+	Ca^{2+}	Fe	As	TN	DOC	PO_4	pH
	mM	mM	mM	μM	μM	mM	mM	mM	
Compost solution	5.83	17.8	1.53	47.3	0.60	4.83	45. 8	17.1	7.45
Electrolyte solution	10.0	25.0	–	–	–	–	–	–	4.5[a]

Tailings were from top 25 cm of Iron King mine Humboldt Smelter Superfund Site, in central AZ, USA. Compost was commercially available organic plant and manure waste. Compost solution was extracted and filtered from 1:10 in DI water, the electrolyte solution was 10 mM NaCl + 25 mM KCl to match the background ionic strength of the compost. TN = total nitrogen, TC = total carbon, TS = total sulfur, BDL = below detection limit, [a] pH adjusted to 4.5 with HCl and NaOH.

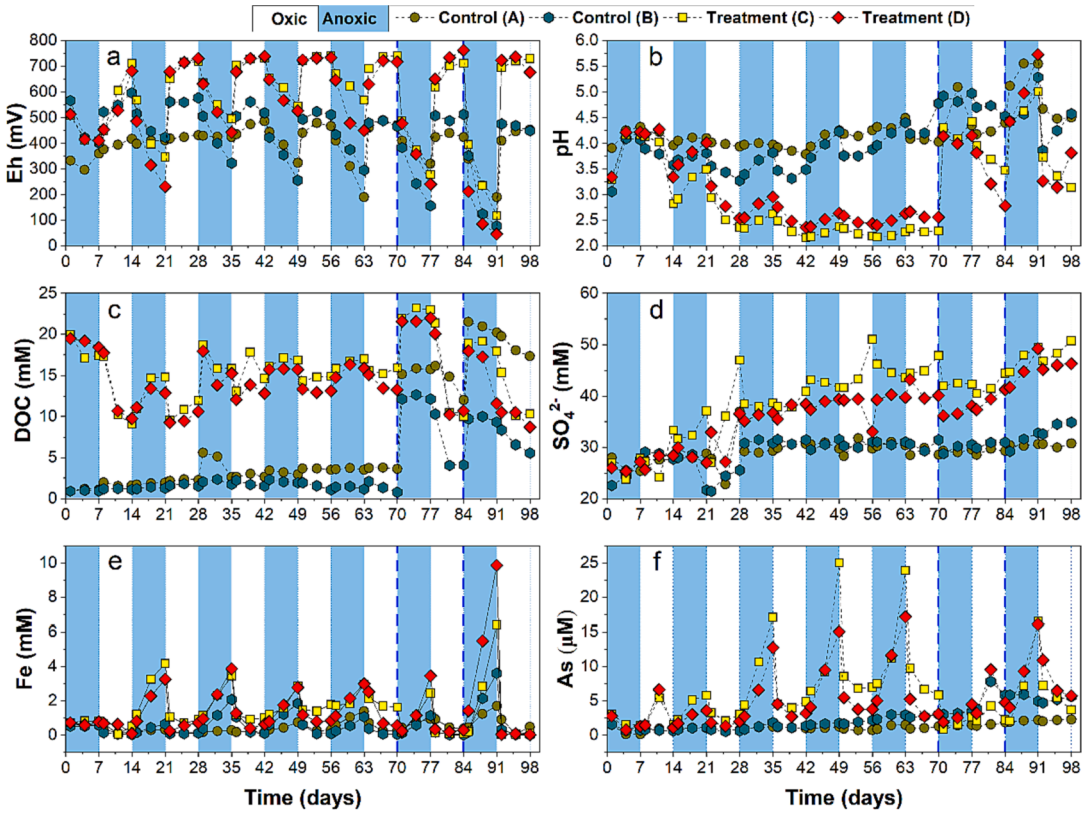

Fig. 1. Aqueous chemistry measured as a function of time in the duplicate Treatment (compost solution added) and Control (compost-free) reactors: (a) Eh, (b) pH, (c) DOC, (d) SO_4^{2-}, (e) total Fe, (f) As. The dashed blue line indicates at day 70 (onset of 6th anoxic half-cycle) and 84 (onset of 7th anoxic half-cycle), 0.25 g glucose was added to reactors and pH was adjusted to 4.5 with NaOH.

of labile C, initially as dissolved compost in Treatment reactors and later as glucose in all reactors, substantially elevated the fraction of As(III). Additionally, arsenobetaine and dimethylated As were detected in the Treatment reactors. Geochemical modeling showed that arsenate as $H_2AsO_{4\,(aq)}^-$ and $H_3AsO_{4(aq)}$ dominated solution species from both groups.

The molar As:Fe ratio decreased (increased) during anoxic (oxic) half-cycles in the Controls, whereas this trend was not evident in Treatment reactors (Fig. 3). Most samples displayed lower As:Fe than that of unreacted t_0 tailings (0.025) and of the AAO extractable fraction (0.039). These results suggest that mechanisms of As release differ between Control and Treatment groups.

During anoxic half-cycles, the concentrations of dissolved As and Fe are correlated (Fig. 4a). Furthermore, dissolved As and As (III) had a significant and positive relationship with Fe^{2+}, respectively (Fig. 4b, c). The Pearson correlation coefficients of As vs Fe, As vs Fe(II), and As(III) vs Fe(II) in treatment groups were higher than that in control groups.

During anoxic half-cycles, the concentration of Fe had a positive correlation with pH in the control groups ($r = 0.411$, $p < 0.01$) and treatment groups ($r = 0.411$, $p < 0.01$) (Fig. 5a). The concentration of As had a positive correlation with pH in the control groups ($r = 0.449$, $p < 0.01$) and a negative correlation with pH in the treatment groups ($r = 0.313$, $p < 0.05$) (Fig. 5b).

3.3. Single and Selective extractions

Results of the 0.5 M HCl extraction are given in Fig. 6 (details in Table S2). Extraction of ferrous Fe was primarily Fe^{2+} adsorbed at the solid surface. Extractable Fe^{2+} increased in anoxic half-cycles and decreased in oxic half-cycles. The Controls presented higher concentrations of Fe^{2+} than did the Treatments, particularly after the third full cycle. Adsorbed Fe^{2+} remained mostly constant for Treatments and tended to increase by the end of the experiment, after glucose addition (Fig. 7a). Extracted total Fe, defined here as deriving from the SRO Fe solids that were solubilized in 0.5 M HCl, was above 100 mmol kg^{-1}, and it increased during oxic half-cycles and decreased during anoxic half-cycles, inverse to the trends for $[Fe]_T$ and consistent with variation in the saturation index for ferrihydrite (Fig S4). The mass of As extracted by 0.5 M HCl decreased in all reactors across the duration of the experiment (Fig. 7b), indicating decreasing arsenic lability with increasing redox fluctuations.

The NaH_2PO_4 extractable Fe was very low (ca. 10 mmol kg^{-1}). The AAO-extractable Fe in Treatments was higher than in Controls, and showed a small increase with time, whereas Controls showed a decrease (Fig. S5). The AAO-extractable Fe in the Treatments increased from 679 mmol kg^{-1} at t_0 to 911 ± 30 mmol kg^{-1} at day 98, whereas AAO-extractable Fe in the Controls decreased from 615 to 520 ± 30 mmol kg^{-1} over the same time frame (Fig. 8). The CBD-extractable Fe increased with time in all reactors, and it represented a larger fraction of the total extractable Fe in the Controls despite being a smaller absolute mass. In the Controls, CDB-extractable Fe increased from 744 mmol kg^{-1} at t_0 to 1129 ± 114 mmol kg^{-1} at day 98, whereas in Treatments it increased from 731 to 942 ± 10 mmol kg^{-1} over the same time frame. There were no detectable intra-cycle trends for the sequential extractions (Fig. 8).

The arsenic removed in the CBD-extraction increased slightly over the seven full redox cycles in both Controls and Treatments, with larger increases in the Controls, whereas AAO-extractable As was not significantly changed. For example, CBD-extractable As was <3 mmol kg^{-1} in all reactors at the start of the experiment, at 98 d, it rose to 9.54 ± 1.88 mmol kg^{-1} in the Controls and 6.94 ± 0.37 mmol kg^{-1} in the Treatments (Fig. 9). Conversely, AAO-extractable As values remained close to 24 mmol kg^{-1} throughout the experiment. There were no evident differences between samples taken immediately following anoxic versus oxic

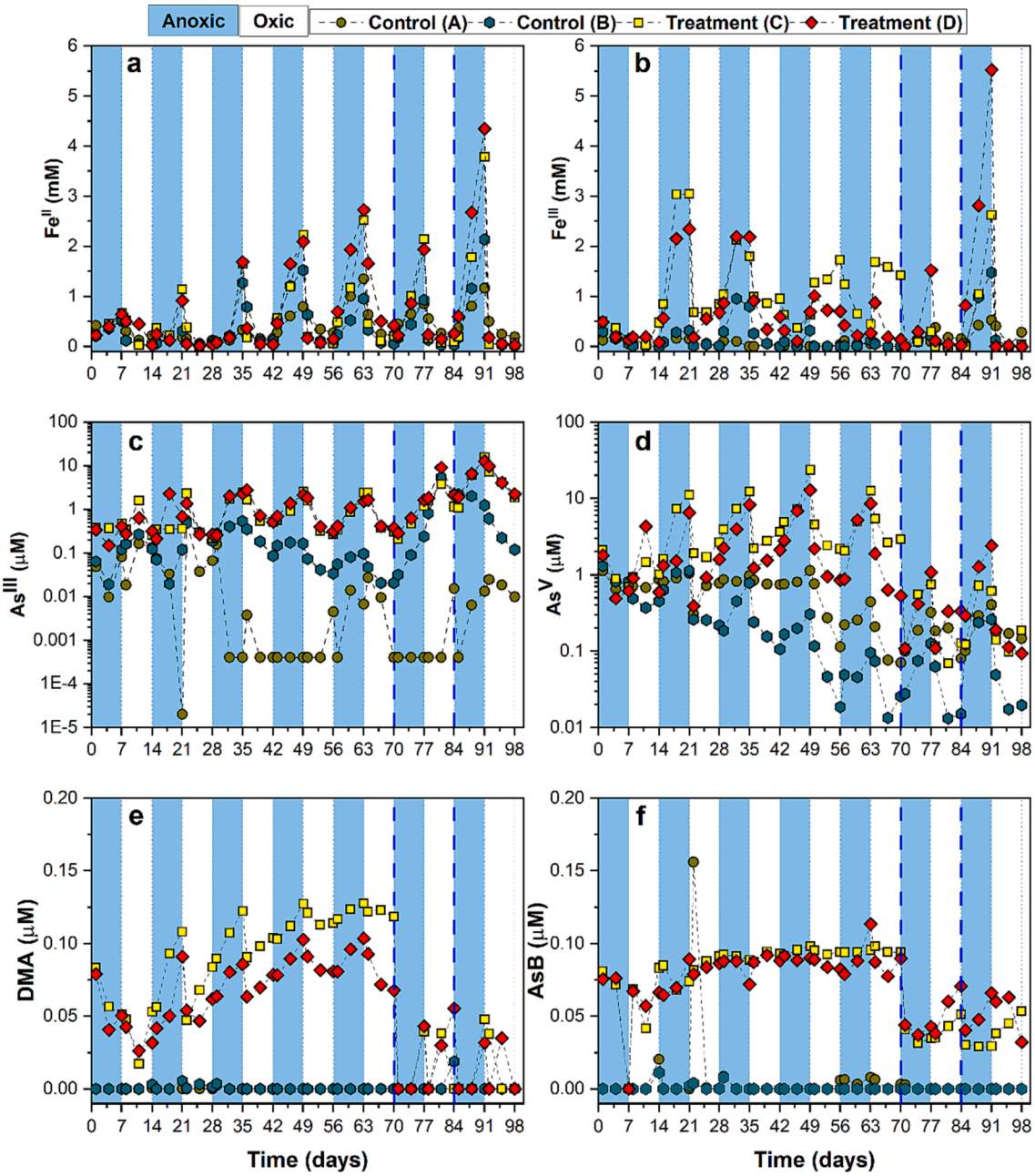

Fig. 2. Speciation of aqueous phase Fe and As during redox cycling over 98 d. Blue and white highlighting indicates anoxic and oxic conditions, respectively. Arsenic concentration (μM) is shown on log-scale. Limit of detection for As^{III} was 0.001 μM. The dashed blue vertical lines indicate at day 70 (onset of 6th anoxic half-cycle) and 84 (onset of 7th anoxic half-cycle), 0.25 g glucose was added to reactors and pH was adjusted to 4.5 with NaOH.

half-cycles. The NaH_2PO_4-extractable As decreased in the Controls at the end of the experiment (from 7.11 mmol kg^{-1} to 2.42 ± 0.91 mmol kg^{-1}), but it was relatively constant in the Treatments (from 5.28 mmol kg^{-1} to 4.93 ± 0.07 mmol kg^{-1}).

3.4. X-ray diffraction and X-ray absorption data

Significant changes in XRD peak intensities were not observed for several of the major crystalline minerals (e.g., quartz, and gypsum) over the course of the experiment, but treatment effects on pyrite abundance were evident. Specifically, pyrite peaks weakened from the Treatments but not from the Controls (data shown for Control B and Treatment C in Fig. 10). The quantitative calculation showed that jarosite increased and pyrite decreased in Treatment C with increasing cycles (Table 2). The Fe XAS result further confirmed the XRD results, it showed that jarosite increased from ~62% in initial tailings to ~78% in the final tailings, whereas pyrite (9–3.2%) and ferrihydrite (29–19%) significantly decreased (Fig. 11). The Arsenic K-edge XANES results (Fig. 12) indicate that only As(V) is detectable in the solid samples during both anoxic and oxic half-cycles.

4. Discussion

4.1. Pyrite oxidation in reactors with compost solution

Pyrite and arsenopyrite are the major S, Fe, and As hosts in unweathered deep tailings (>180 cm) from IKMHSS, accounting for 95% of the S, 71% of the Fe, and 100% of the As (Hayes et al., 2014; Root et al., 2015). In the surficial weathered tailings used in the current experiments; however, these sulfides have been largely transformed via

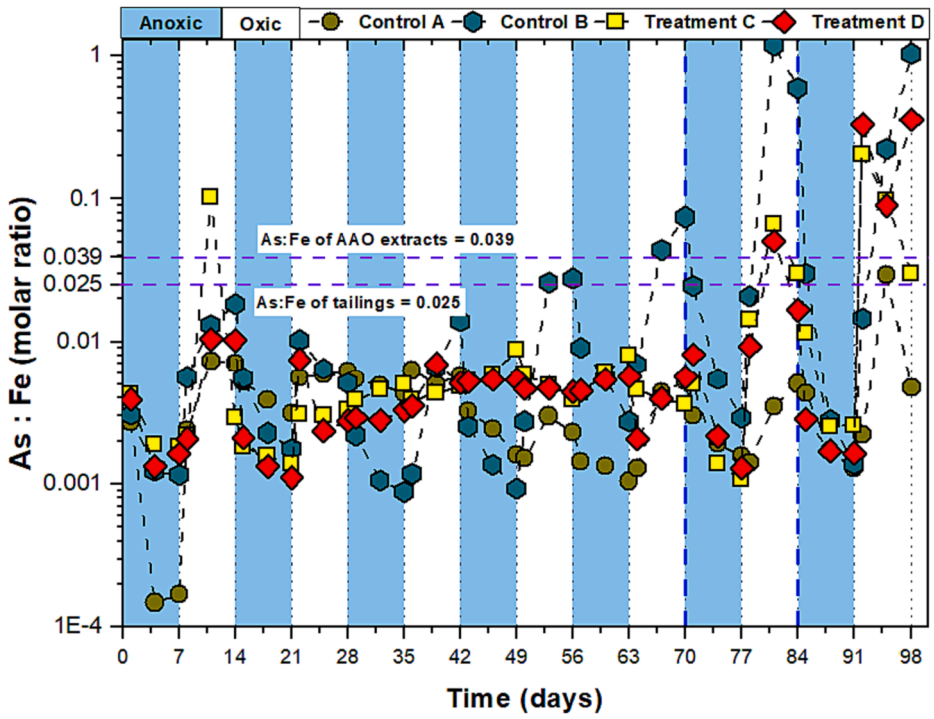

Fig. 3. Molar As:Fe ratio of aqueous reactor solutions in the absence (A, B) and presence (C, D) of compost solution over the course of the experiment. Blue and white highlighting indicates anoxic and oxic conditions, respectively. Horizontal dashed lines show As:Fe ratios *at* t_0 (0.025) and from AAO extracted (0.039) tailings.

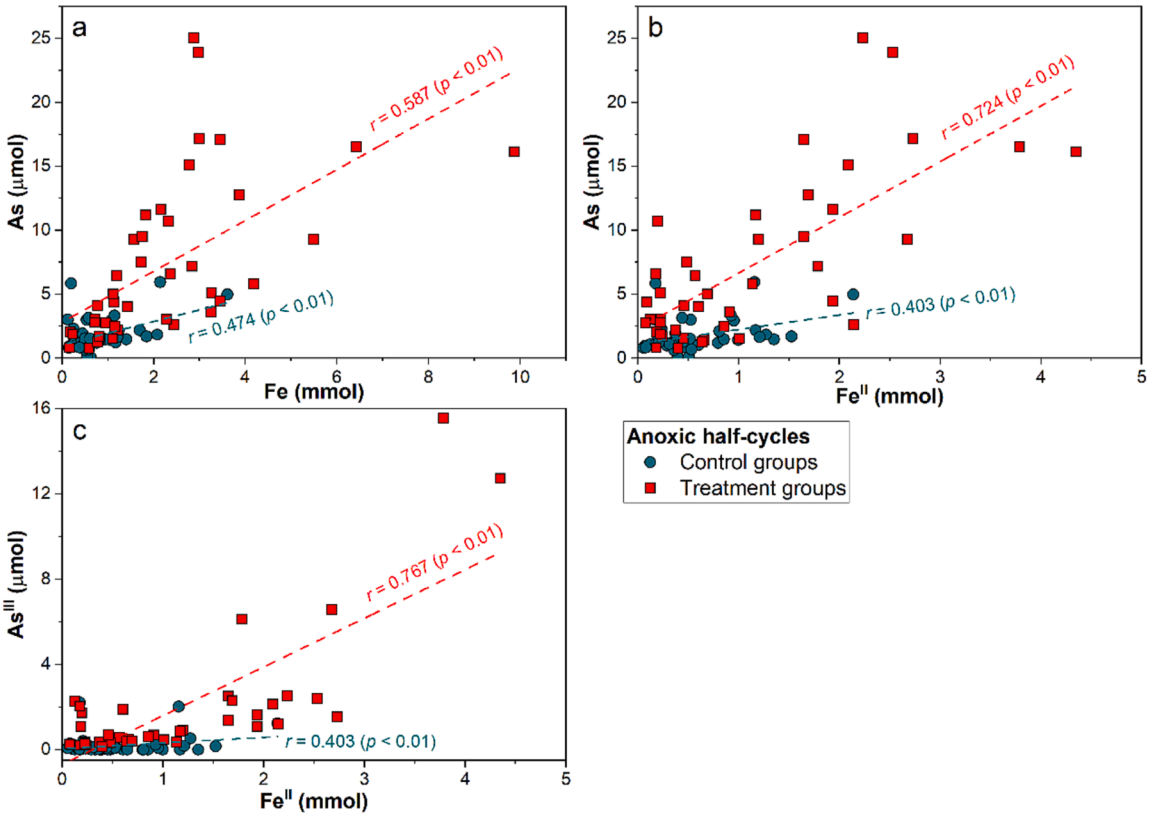

Fig. 4. Dissolved As vs Fe (a), As vs Fe(II) (b), and As(III) vs Fe(II) (c) during anoxic half-cycles. Dashed lines are linear fits, r = Pearson's correlation coefficients shown where $p < 0.01$.

oxidation to secondary minerals ferrihydrite and jarosite that contain either adsorbed or structural As, and only a minor fraction of pyrite (~5%) remained in the near surface (Table 2). The larger increase in SO_4^{2-} and proton activity (Fig. 1) combined with the loss of pyrite (Fig. 10d, Table 2) in Treatment reactors indicates that the residual pyrite was oxidized more quickly in reactors containing compost

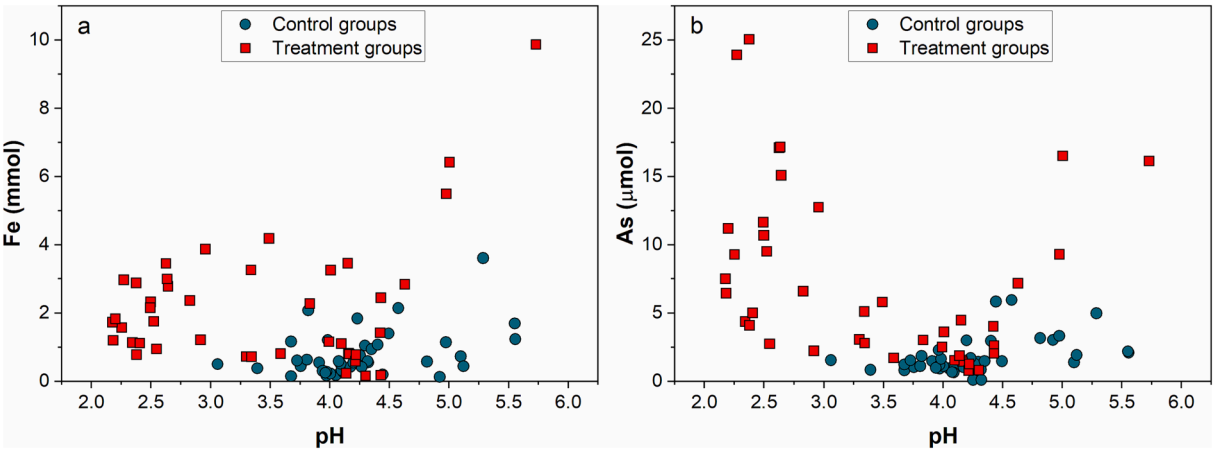

Fig. 5. Aqueous Fe (a) and As (b) as a function of pH under anoxic half-cycles in bio-reactors.

solution, and this explains the mineralogical transformation observed (Fig. 10d). Assuming the increase in SO_4^{2-} (~20 mmoles) originated from pyrite weathering, approximately 10 mmoles of FeS_2 (~1.2 g) were oxidized, which is 2.4% of the 50 g tailings mass used in the experiment, consistent with the variance in calculated pyrite content within error (Table 2). Abiotic oxidation of pyrite by $O_{2(aq)}$ may not be the case in our study, since pyrite oxidation was not observed even though the Control reactors were purged with air for 7 d during each of the 7 cycles (Fig. 1, Fig. 10b, Table 2). Soluble Fe^{3+}, rather than $O_{2(aq)}$ is the dominant oxidant for pyrite under acidic conditions (pH < 4) (Evangelou and Zhang, 1995; Nordstrom, 2011). The high soluble Fe^{3+} concentration observed in the Treatment reactors (e.g., an average of 0.70 mM in oxic half-cycles in Treatment C) therefore likely contributed to the oxidation of pyrite, and the lower pH conditions observed. Conversely, in the Controls, soluble Fe^{3+} in oxic half-cycles was at or below the limits of detection (Fig. 2).

Microbial activity is likely a critical factor contributing to the oxidation of pyrite in the presence of compost OM solution. A previous study of IKMHSS tailings reported Fe- and S-oxidizing bacteria and archaea including *Thiomonas*, *Thiobacillus*, *Sulfobacillus*, *Alicyclobacillus*, *Acidithiobacillus*, *Leptospirillum* and *Ferroplasma* in the tailings from IKMHSS (Valentín-Vargas et al., 2018). Among these, *Acidithiobacillus* and *Ferroplasma* are regarded as not only Fe/S-oxidizers but also Fe/S-reducing microorganisms (Schippers et al., 2010; Ziegler et al., 2013). Their metabolic activities include aerobic Fe^{2+} oxidation and anaerobic Fe^{3+} reduction using Fe(III) as a terminal electron acceptor, and they may gain energy from labile organic carbon (Schippers et al., 2010; Ziegler et al., 2013). Therefore, the reductive dissolution of amorphous iron oxides in tailings under anoxic half-cycles resulted in elevated concentrations of Fe^{2+}. Under an acidic environment, the Fe^{2+} can be re-oxidized by iron-oxidizing microorganisms (Ziegler et al., 2013), and soluble Fe^{3+} then acted as an oxidant of pyrite. Additionally, the compost solution provided nutrients and DOM to stimulate microbial growth. Soluble reduced carbon could provide energy for heterotrophic bacteria, including Fe-reducing strains that would be activated during the anoxic half-cycles, and the mineralized carbon (CO_2) coupled with elevated Fe^{2+} are expected to facilitate the growth of Fe oxidizing bacteria, thereby accelerating pyrite oxidation. Although the addition of compost could provide microbial inoculum (Mendez et al., 2007; Solís-Dominguez et al., 2012; Nelson et al., 2015), this effect was limited due to 1 μm pre-filtration of the compost solutions. Interestingly, an increase in the abundance of *Acidithiobacillus* in compost amended tailings was observed in a greenhouse mesocosm experiment (Valentín-Vargas et al., 2018). Moreover, increased pyrite oxidation during compost amendment was also observed during a three-year phytostabilization study conducted at IKMHSS, where the same compost was added as an amendment (Hammond et al., 2020). Hence, in this way, biological enhancement of pyrite oxidation in the presence of soluble organic matter altered reactor geochemistry (pH, soluble sulfate, and secondary Fe minerals), which, in turn, controlled the portioning of As between the solid and aqueous phase.

4.2. Mechanism of As release and retention

4.2.1. Mobilization of As in anoxic half-cycles

Mobilization of As during anoxic half-cycles was stimulated by the presence of compost solution and was essentially undetectable in the Controls until the addition of glucose at day 70 (Fig. 1). This is similar to the results obtained in batch experiments (Bozeman, 2018). Dissimilatory Fe reducing microorganisms (DIRMs) – heterotrophic bacteria and archaea that use Fe(III) as a terminal electron acceptor in respiration (Lovley, 1991) – coupled with the presence of labile organic matter, were likely important factors controlling As mobilization. As mentioned above, *Acidithiobacillus* and *Ferroplasma* observed in these tailings are facultative anaerobes that can utilize Fe(III) as a terminal electron acceptor during oxidation of organic carbon (Schippers et al., 2010; Ziegler et al., 2013; Valentín-Vargas et al., 2018). SRO Fe minerals, characterized by high specific surface area, poor crystallinity, and high reactivity are the preferred DIRM sources of Fe^{3+} (Thompson et al., 2006; Aeppli et al., 2019), and they accounted for a large mass fraction of Fe and As in the tailings. Approximately 50% of the total Fe and 70% of the total As was solubilized with SRO during the AAO extraction step (Figs. 8 and 9). This provided a large pool of reducible Fe for DIRM in the reactors. However, organic substrates in these tailings were extremely low, so added labile carbon was a key factor controlling reductive dissolution of Fe minerals and mobilization of As. Lack of labile carbon limited heterotrophic microbiological activity in the Controls, where only a small fraction of Fe was reduced, accompanied with trace As mobilization (Fig. 1). An inverse relation was noted for DOC and pH, where low DOC was associated with higher pH. This situation changed after extra glucose addition, which elevated Fe reductive dissolution and increased As mobilization, even in the Control reactors. In a previous study, Parsons et al. (2013) found that As release during anoxic half-cycles tended to decrease with increasing cycles, since their system was oscillated without an external reduced carbon source, and thus the DOC was gradually depleted with increasing time. In reactors treated with compost solution, high concentrations of DOC (~20 mM) stimulated heterotrophic microbial activity, which in turn increased reductive dissolution of SRO Fe and simultaneous As mobilization during anoxic half-cycles (Fig. 1). The significantly positive correlation of total As vs total Fe ($r = 0.587$, $p < 0.01$) and total As vs Fe(II) ($r = 0.724$, $p < 0.01$) (Fig. 4), combined with 78 ± 6% of As(V) in Treatments over the first five cycles (Fig. 2), supported the release of As by reductive dissolution of Fe. However, the release of Fe and As was decoupled after the second

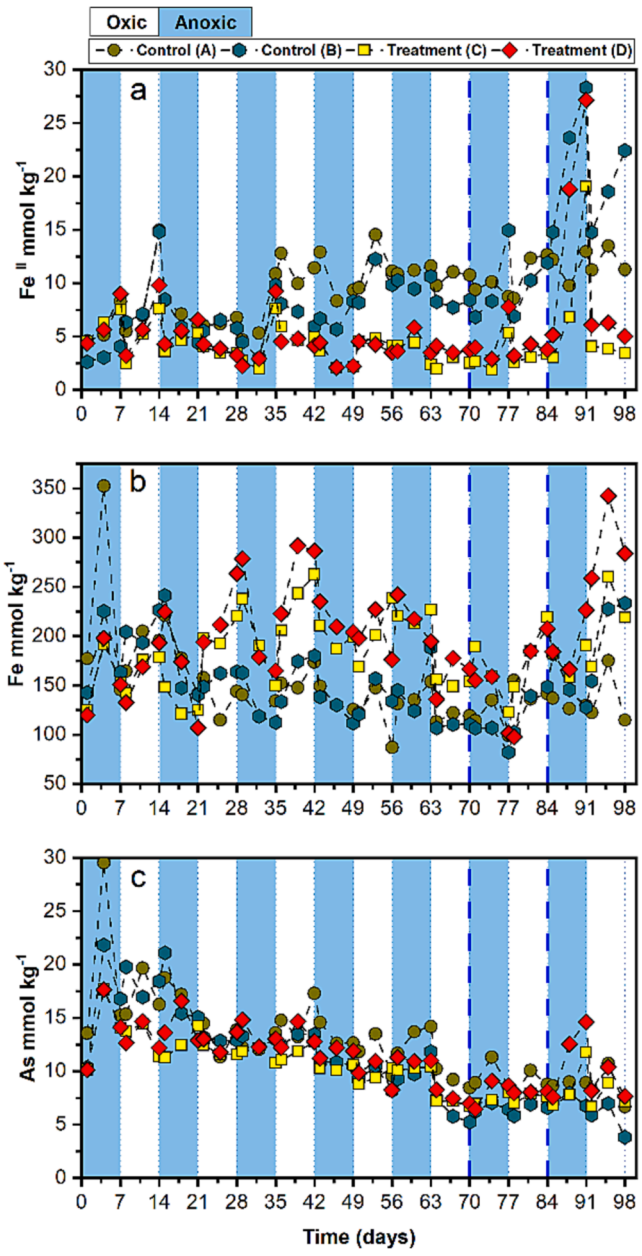

Fig. 6. The concentrations of 0.5 M HCl-extractable Fe(II), Fe and As in solid samples during redox cycling over 98 d. Blue and white highlighting indicates anoxic and oxic conditions, respectively. The dashed blue vertical lines indicate at day 70 (onset of 6th anoxic half-cycle) and 84 (onset of 7th anoxic half-cycle), 0.25 g glucose was added to reactors and pH was adjusted to 4.5 with NaOH.

cycle; aqueous As tended to increase with increasing cycles whereas aqueous Fe slightly decreased, accompanied with an increase in SO_4^{2-} and decrease in pH. These results indicate that other processes contribute to the mobilization of As from tailings.

The increase in As(III) during anoxic half-cycles in Treatment reactors indicated that arsenate reduction may contribute to the mobilization of As in tailings porewater. Moreover, dissolved As(III) concentration was much higher in Treatments than Controls, particularly after addition of labile carbon (Fig. 2). Arsenate reduction is generally related to microbial activities via respiratory and/or detoxification pathways (Campbell et al., 2006). It is reported that the threshold for expressing the *ars* detoxification genes is As(V) > 100 μM, but it is only 100 nM for the expressing of *arr* respiratory genes (Saltikov et al., 2005). The dissolved As(V) in our reactors (< 24 μM) was far less than the threshold for expression of *ars* genes. Based on the variance in soluble As(III) in our reactors (Fig. 2), we speculate that the respiratory pathway coupled with oxidation of organic carbon is probably the dominant mechanism of As(V) reduction. Previous studies found that some Fe and S reducers can also mediate dissimilatory reduction of As adsorbed by ferrihydrite (Zobrist et al., 2000; Islam et al., 2004; Jiang et al., 2013). Additionally, organic compounds solubilized from the compost may act as an electron shuttle to promote As reduction in anoxic environments (Qiao et al., 2019). The uncharged arsenite, As $(OH)_3^0$, is more mobile than As(V) and sorption to ferrihydrite at acidic pH values, as were maintained in this study, is negligible (Dixit and Hering, 2003). This is consistent with the As XAS results, which show that As in the solids was predominantly As(V) (Fig. 12). Similarity in the trends of Fe(II) and As(III) (Fig. 2), together with the significantly positive correlation between Fe(II) and As(III) in Treatment reactors under anoxic half-cycles ($r = 0.767$, $p < 0.01$), suggests that Fe and As were likely reduced simultaneously. Aqueous speciation analysis included organic arsenic analysis, and trace organic As was observed in the Treatment group (Fig. 2), consistent with the compost-induced stimulation of microbial activity and production of As metabolites.

Dissolved OM can also affect As mobilization through abiotic pathways via competition for reactive ferrihydrite surface sites (Evanko and Dzombak, 1999; Mladenov et al., 2015). Because ~50% of the DOC was indeed adsorbed by tailing solids after 24 h, organic anions were competing with As for the sorption sites and promoting As release (Bauer and Blodau 2006). Additionally, high phosphate (PO_4^{3-} ~ 17 mM) was observed in the compost solution (Table 1) and the NaH_2PO_4 extractable As was lower in the Treatment group than that in Control group (Fig. 9) suggesting that phosphate was competing with arsenate for adsorption to tailing particles (Goh and Lim, 2005; Bozeman, 2018). In summary, the results indicate that compost drives As reduction (and to a smaller extent, methylation) in tailings, and competes for reactive iron surface sites, processes that increase As mobility and would contribute to downward (and/or lateral) translocation in field sites. Additionally, although direct release of As from pyrite oxidation induced by compost solution is not expected since As was absent in pyrite (Fig. 12, Root et al., 2015), the associated proton production can promote the dissolution of Fe minerals and release of As into solution (Panias et al., 1996; Wiederhold et al., 2006). The pH in Treatment reactors dropped to ~2.2 by the third redox cycle, and the extremely low pH likely explains the low Fe^{2+}adsorption by tailings (Fig. 6). This pH value is similar to the pK_{a1} (2.20) of H_3AsO_4 (O'Day, 2006), and thus decreased the adsorption ability of arsenate since it may be protonated. Comparing aqueous Fe and As as a function of pH suggests such an effect in Treatment reactors (Fig. 5), which showed high soluble As at low pH (< 3.0) under anoxic (Fig. 5b) conditions. At the IKMHS tailings field site, the compost-buffered pH dropped about 2 units after 3 years under 15% by mass amendment, but the pH change under 20% by mass compost amendment was very small (Gil-Loaiza et al., 2016). These results suggest that a suitable amendment rate should be considered based on the buffer capacity of compost and the acidification potential from pyrite oxidation.

4.2.2. *Immobilization of As*

Most of the As released during anoxic batch reactor half-cycles was immobilized in the following oxic half-cycle, concurrent with the oxidation of Fe(II) and As(III) (Figs. 1 and 2). In all reactors, the 0.5 M HCl extractable Fe significantly increased during oxic half-cycles, and this effect was more pronounced in the compost Treatment group. The increase in 0.5 M HCl extractable Fe indicated precipitation of neoformed SRO Fe minerals (Fig. 6), similar to previous redox oscillation experiments conducted on soils (Thompson et al., 2006; Parsons et al., 2013; Phan et al., 2019). Fe(II) can be oxidized abiotically by O_2 and/or biotically by Fe/S-oxidizers that dominate the microbial community in these tailings (Valentín-Vargas et al., 2018). Generally, the stability of

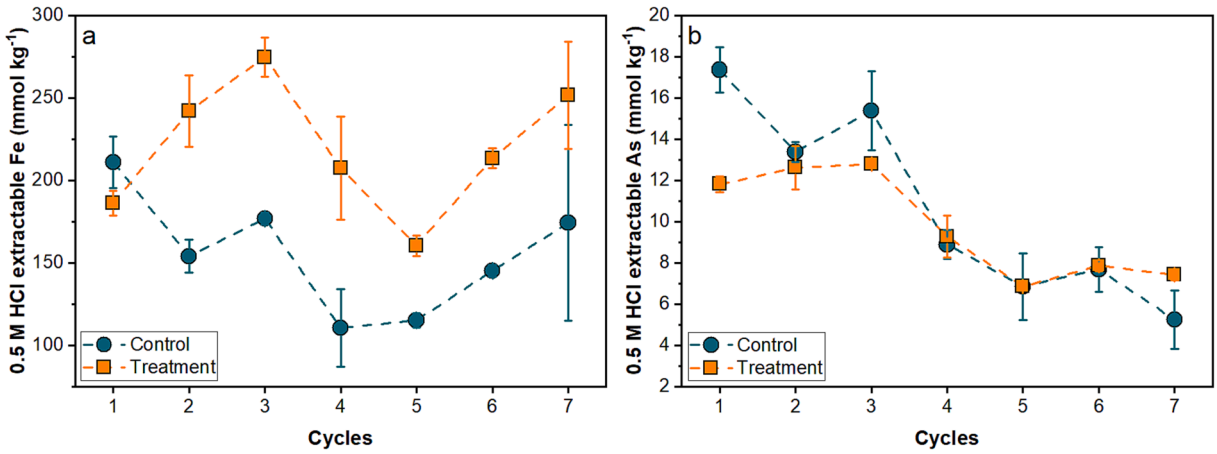

Fig. 7. The 0.5 M HCl extractable Fe (a) and As (b) from tailing solids after each redox full cycle. Extractable As decreases with increased cycling under control and compost treatment.

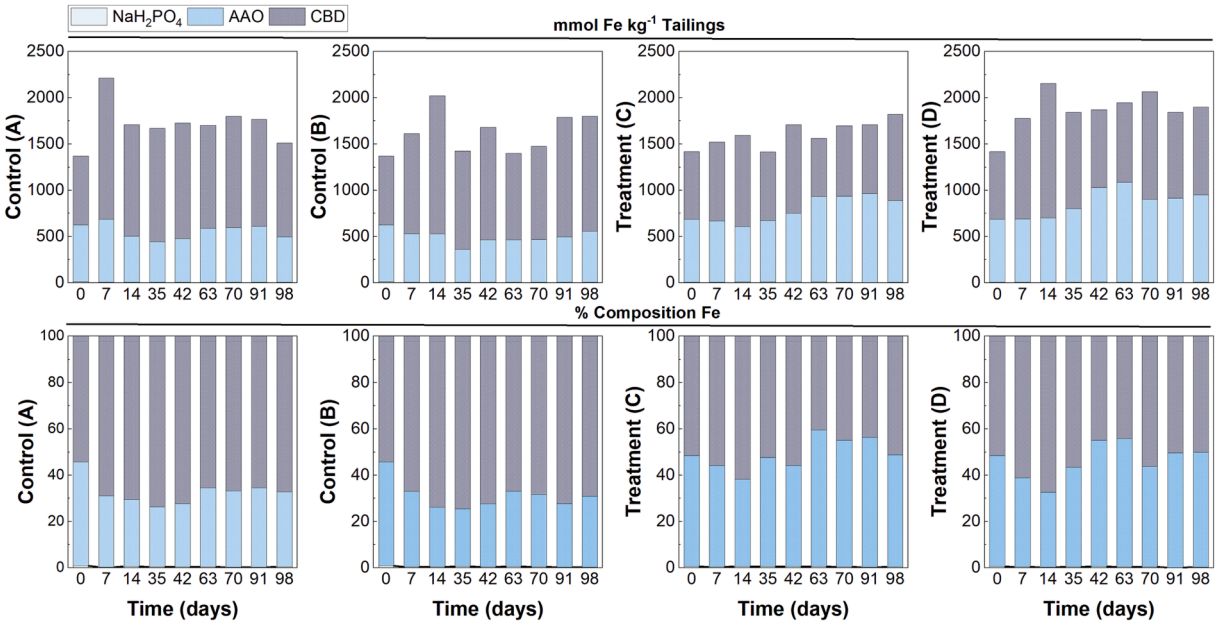

Fig. 8. Release of Fe by selective sequential extraction, displayed as both molar concentration (top) and normalized percent (bottom). Extraction steps were 1 M NaH_2PO_4, 0.2 M AAO, and CBD (modified from Hayes et al., 2014). Negligible Fe was released by NaH_2PO_4 under either experimental condition.

aqueous As(III) should exceed 25 h without preservation (Bednar et al., 2002), the addition of $O_{2(g)}$ itself would not be sufficient to account for the amount of As oxidation over a short time (< 24 h). However, the presence of Fe(II) in solutions purged with air can stimulate the co-oxidation of As(III) with Fe(II) by producing reactive oxidants such as Fe(IV) species (Hug and Leupin, 2003; Roberts et al., 2004). Moreover, *Thiomonas* spp. observed in the tailings, can also utilize arsenic as an electron donor to generate energy and thus likely mediated the oxidization of As(III) (Duquesne et al., 2008; Valentín-Vargas et al., 2018). Notwithstanding the limit of XAS detection of As(III), only As(V) was detected in the tailing solids, suggesting As(III) was oxidized to As(V) as a surface complex. This indicates that microbial mediation resulted in As (V) being immobilized as adsorbed and/or occluded with freshly precipitated SRO Fe minerals, such as ferrihydrite, that are high affinity adsorbents for oxyanion As(V) where ferric hydroxide surface sites are protonated at low pH (Dixit and Hering, 2003).

An additional pathway for As sequestration is by incorporation of arsenate into the tetrahedral (T_d) site of jarosite as a substitute for sulfate (Karimian et al., 2017). The physicochemical environment of the solutions during most oxic half-cycles, i.e., high acid (pH < 3), high ferric iron (up to 1.7 mM) and sulfate activity (> 20 mM), would favor the formation of jarosite (Asta et al., 2009). Indeed, geochemical modeling indicated that solutions were supersaturated with respect to jarosite due to high H^+, K^+ and SO_4^{2-} activity. This was supported by the increase in jarosite with increasing redox cycles (Figs. 10, 12, Table 2). The sequestration of As in jarosite is evidenced by the higher content of CBD-extractable As at the end of the experiment than that in the initial samples, while AAO-extractable and NaH_2PO_4 As were slightly decreased (Fig. 5). Although the pH and SO_4^{2-} content in our reactors may also favor the precipitation of schwertmannite (Bigham et al., 1996; Acero et al., 2006), neither Fe XAS nor XRD detected schwertmannite in reacted tailings. This is probably related to the extremely low pH (< 3), as schwertmannite is commonly formed in the pH range 3.0–4.5 (Bigham et al., 1996). Hence, while compost amendment may induce reductive mobilization of As in anoxic tailings in field sites, the released As is subsequently immobilized via adsorption to ferrihydrite and/or incorporated into jarosite under oxic cycles, limiting As efflux (Hammond et al, 2020).

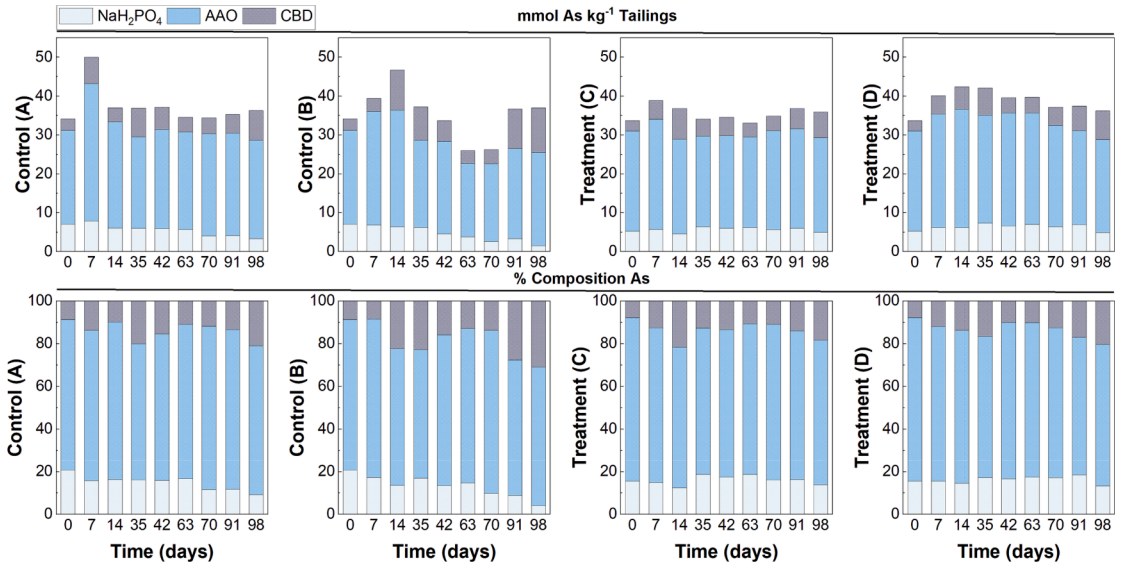

Fig. 9. Release of As by selective sequential extraction, displayed as molar concentration (top) and normalized percent (bottom). Extraction steps were 1 M NaH_2PO_4, 0.2 M AAO, and CBD (modified from Hayes et al., 2014). Both treatments showed that repeated redox cycles decreased As released by NaH_2PO_4 and under compost treatment CBD extractable As decreased relative to the control.

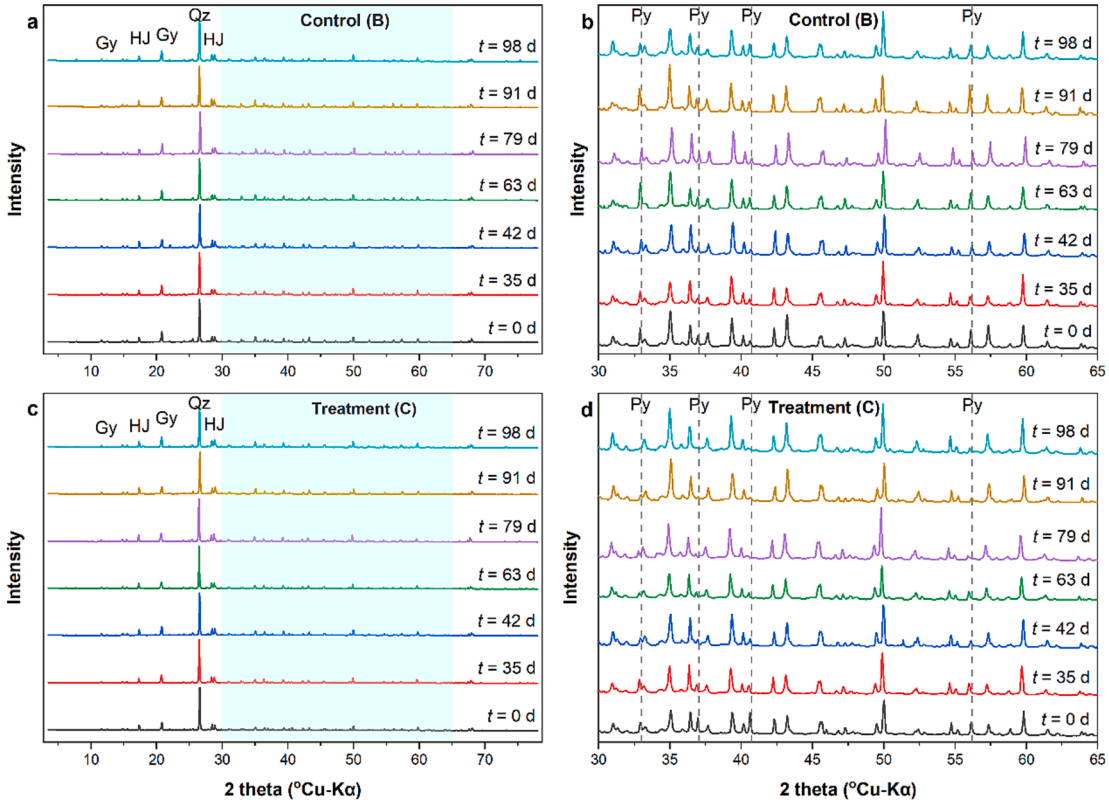

Fig. 10. X-ray diffraction results from Control (B) and compost treated Treatment (C) bioreactors. Diffractograms are normalized to quartz $(1\ 0\ 1)_{hkl}$ at 26.6° 2θ (d = 3.34 Å). (Qz: Quartz; Gy: Gypsum; HJ: Hydronium jarosite; Py: Pyrite). Full diffractograms are given left (a, c); zoomed in sections (30–65 °2θ) are from highlighted sections to show pyrite peaks (b, d).

The initial sulfur speciation in the surface tailings consisted of gypsum, jarosite and pyrite (Hayes et al., 2014). In anoxic half-cycles, there was no significant decrease in dissolved sulfate, and geochemical modeling showed that the activity of S^{2-}, HS^- and other reduced S species was vanishingly low in all solutions. This result is consistent with a previous study that showed that [S^{2-}] at near detection limits under similar redox cycling experimental conditions in delta sediments (Phan et al., 2018). The extremely low pH (~3), low organic carbon (~0.1%), and the semi-arid climate of the sampling site, most likely restrains the presence of sulfate reducing bacteria (SRB) that prefer an environment with pH > 5 (Koschorreck, 2008). This was evidenced by a previous study of the same tailings in which SRB were not observed in original tailings and tailings amended with compost (Valentín-Vargas et al., 2018). Additionally, the acidic pH and high available Fe^{3+} also inhibit

Table 2
Quantitative XRD results of the crystalline mineral phases in the samples from Rietveld refinement.

t (d)	H^+ Jarosite	Gypsum	Quartz	Pyrite	Corundum	Chlorite	G.O.F.[a]	Crn. Std.[b]
Reactor B								
0	14.7	10.8	44.8	4.4	22.4	3.0	0.8	16.3
35	17.7	10.9	51.6	3.5	13.4	2.8	0.4	12.0
42	19.3	11.6	51.3	3.3	14.5	0	1.6	13.9
63	15.8	8.9	48.5	5.8	19.1	2.0	0.2	14.7
79	15.2	10.9	47.7	3.6	20.8	1.9	0.4	18.0
91	18.6	7.6	46.6	5.5	18.6	3.0	0.2	13.6
98	17.4	15.2	51.6	4.4	11.3	0	1.5	11.4
Reactor C								
0	18.3	9.7	55.1	5.4	11.4	0.1	0.9	11.6
35	17.5	10.8	52.5	4.0	13.2	2.0	1.9	11.7
42	20.7	12.1	45.9	2.0	15.2	4.1	0.3	12.3
63	21.4	11.2	48.9	2.3	15.2	1.0	0.4	12.8
79	22.2	14.3	51.3	1.6	10.7	0	3.0	13.1
91	20.6	12.3	46.4	1.2	19.4	0	0.3	15.7
98	21.2	13.5	45.7	0.8	16.8	2.0	1.9	14.1

XRD Rietveld refinement does not include amorphous or poorly crystalline mineral phases. The recovery rate of the corundum (internal standard) ranges from 73% to 122%, with an average of 90%.
[a] Goodness of fit.
[b] Added corundum standard.

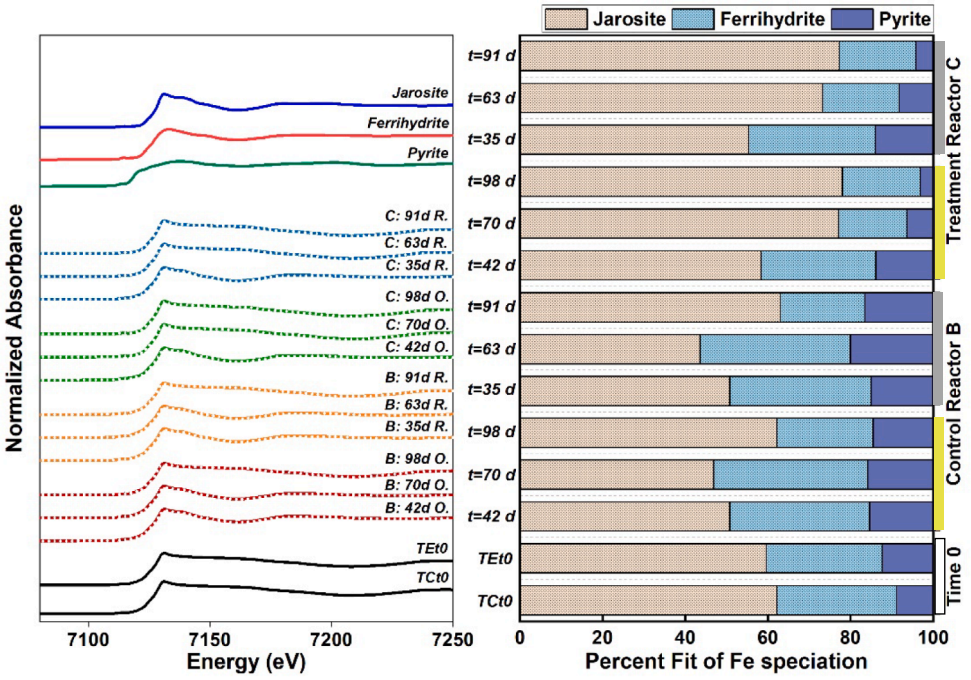

Fig. 11. Linear combination fits of Fe K-edge XANES showing percent components in samples from Control (B) and compost Treatment (C) through time. At the right side, white column indicates time zero samples, yellow column indicates samples from oxic-half cycles and grey column indicates samples from anoxic half-cycles. Data are displayed by solid lines (blue = treated anoxic half-cycles, green = treated oxic half-cycles, orange = control anoxic half-cycles, red = control oxic half-cycles, TBt0 = time zero samples for Controls, TCt0 = time zero samples for Treatments) and linear combination fits are shown by stippled line.

SRB activity (Koschorreck, 2008). Therefore, sulfate reduction was limited, and As immobilization via sulfide precipitation was not expected in our experiment, consistent with the As XAS results showing no detectable As sulfides (Fig. 12).

4.3. Cumulative effects of redox oscillations

Several lines of evidence demonstrate that the speciation of Fe and As in tailings solids changed after 7 full redox cycles. In Control reactors, the 0.5 M HCl extractable Fe generally decreased with increasing redox cycles until extra glucose was added (Fig. 7), accompanied by a slight decrease in AAO-extractable Fe and an increase in CDB-extractable Fe (Fig. 8). The extraction results coupled with Fe XAS and quantitative XRD data confirmed that jarosite was increased at the end of experiment. One of the most important observations of this study was the enhanced oxidization of residual pyrite resulting from compost addition. The release of Fe from pyrite oxidation resulted in an increase in both AAO- and CBD-extractable Fe. These results indicate that the released Fe^{3+} was precipitated as amorphous Fe oxides (e.g., ferrihydrite in this study) and crystalline jarosite as evidenced by the Fe XAS and XRD. Soluble Fe(II) has been demonstrated to drive transformation or recrystallization of ferrihydrite to oxides with longer-range order

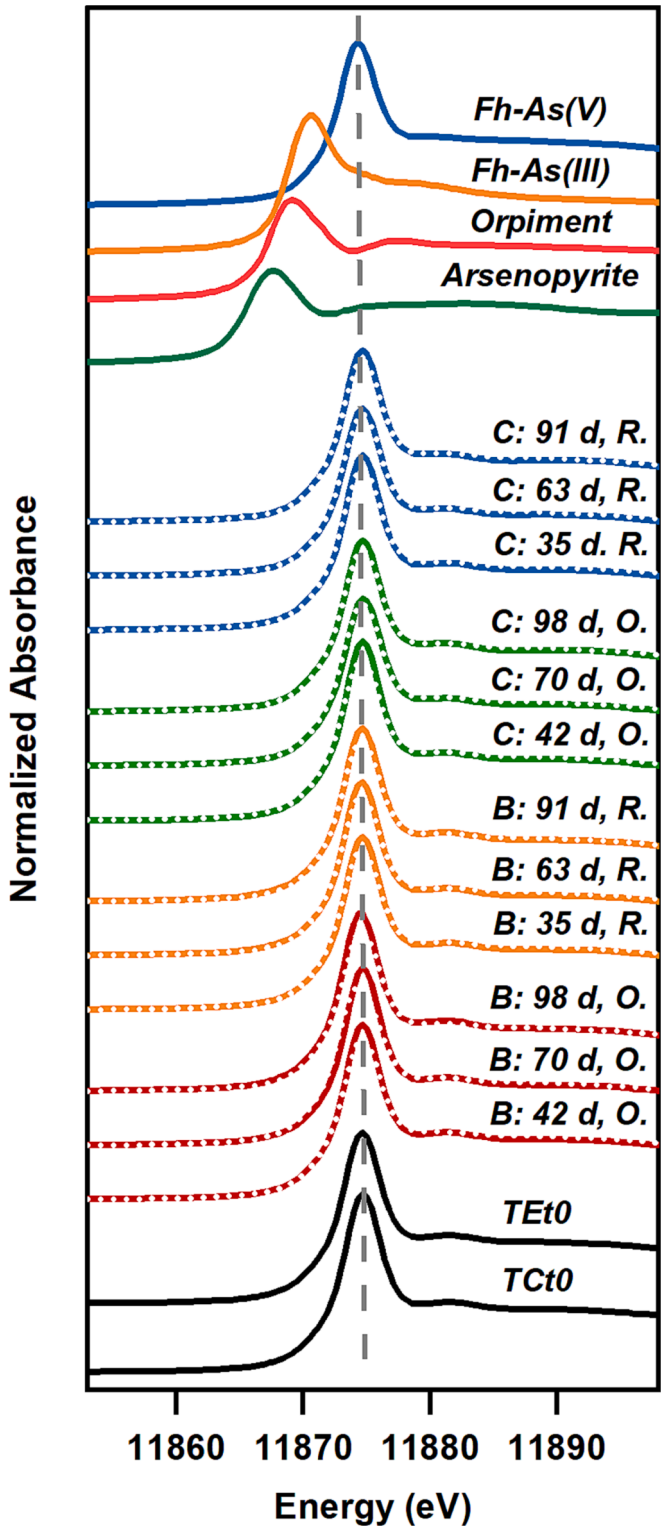

Fig. 12. Normalized As K-edge XANES of samples from Control (B) and compost Treatment (C) through time, reference compounds shown for comparison, Fh-As(V) is ferrihydrite-adsorbed arsenate, Fh-As(III) is ferrihydrite-adsorbed arsenite. Data are displayed by solid lines (blue = treated anoxic half-cycles, green = treated oxic half-cycles, orange = control anoxic half-cycles, red = control oxic half-cycles, TBt0 = time zero samples for Controls, TCt0 = time zero samples for Treatments) and linear combination fits are shown by stippled line. The vertical line indicates the energy position of As(V).

(Hansel et al., 2003; Boland et al., 2014), and it was expected that under anoxic conditions, 0.5 M HCl extractable Fe would decrease. However, this transformation can be poisoned by sorbed As, organic carbon, phosphate, or sulfate (Chen et al., 2015; Karimian et al., 2017), which could explain why goethite and hematite were not detected in this experiment nor in the previous characterization of the tailing samples (Hayes et al., 2014). Collectively, the redox oscillations can result in an increase in jarosite in tailings, since geochemical modeling indicates that some of the dissolved Fe reprecipitates as jarosite under the extremely acidic, sulfate-rich oxic environment. The enhanced pyrite oxidation and increased acid generation in Treatment reactors would promote ferrihydrite dissolution and jarosite precipitation. It is interesting that the 0.5 M HCl- and AAO- extractable As decreased with increasing redox cycles in both Control and Treatment reactors. This was accompanied by an increase in the CBD-extractable As and a decrease in the PO_4^{3-} exchangeable As. These results suggest that As released in anoxic half-cycles was partly co-precipitated in freshly precipitated jarosite in the subsequent oxic-half cycles as mentioned above. Because the migration from tailings to porewater only accounted for 0.01–1.58% of total As, this trace amounts may not be detected by the As XAS.

5. Conclusions

This study reported the dynamics of Fe and As in solution and their biogeochemical transformation in tailing solids in the presence and absence of dissolved compost during a series of seven, two-week-long redox oscillations. The cumulative effects of redox oscillations included a decrease in As lability overall. The presence of compost solution stimulated pyrite oxidation and resulted in decreasing pH and increasing of sulfate in the aqueous phase. The addition of compost solution increased the mobilization of As under anoxic half-cycles through reductive dissolution of SRO Fe minerals, arsenate reduction, and proton promoted dissolution. Microbially-mediated arsenic reduction was observed in the reactors, which increased As mobility due to low affinity of As(III) to ferrihydrite at low pH. Released As was immobilized in subsequent oxic half-cycles due to (co-)precipitation of Fe minerals, especially jarosite. After multiple redox oscillations, the crystallinity of Fe minerals increased in the Control group, and first decreased then increased in Treatment group due to the transformation of Fe minerals. Our results indicate that compost-assisted phytostabilization does not necessarily result in significant translocation of As during reductive excursions because of the re-adsorption and co-precipitation of As that occurs rapidly during the return to oxic conditions. However, residual acid generating potential and adsorptive competition with from DOC need to be considered when managing with compost assisted phytostabilzation.

Declaration of Competing Interest

The authors declare that they have no known competing financial interests or personal relationships that could have appeared to influence the work reported in this paper.

Acknowledgments

We acknowledge support from the National Institutes of Environmental Health Sciences SRP grant P42 ES04940. YL acknowledges funding from the China Scholarship Council (No. 201704910179) and the Youth Innovation Promotion Association of the Chinese Academy of Sciences (No. 2021399). Portions of this research were carried out at Stanford Synchrotron Radiation Laboratory, a National User Facility operated by Stanford University on behalf of the U.S. Department of Energy, Office of Basic Energy Sciences. We thank Mary Kay Amistadi and Daniel Barrientes from ALEC for their analytical and technological support. Prof. Haibo Qin was acknowledged for his help on the Fe XAS data processing.

Appendix A. Supplementary material

The following are the Supplementary material to this article: Map of field collected samples from Iron King Superfund Site, schematic of redox oscillation reactors, plot of calculated saturation index throughout the experiment, plot of selective sequential extraction of As and Fe throughout the experiment, tabulated aqueous chemistry in reactors, tabulated 0.5 M HCl extractions, tabulated three-step sequential extractions, FTIR spectra of DOM used in treatments. Supplementary material to this article can be found online at https://doi.org/10.1016/j.gca.2023.09.012.

References

Abraham, M.R., Susan, T.B., 2017. Water contamination with heavy metals and trace elements from Kilembe copper mine and tailing sites in Western Uganda; implications for domestic water quality. Chemosphere 169, 281–287.

Acero, P., Ayora, C., Torrentó, C., Nieto, J.-M., 2006. The behavior of trace elements during schwertmannite precipitation and subsequent transformation into goethite and jarosite. Geochim. Cosmochim. Acta 70 (16), 4130–4139.

Aeppli, M., Vranic, S., Kaegi, R., Kretzschmar, R., Brown, A.R., Voegelin, A., Hofstetter, T.B., Sander, M., 2019. Decreases in iron oxide reducibility during microbial reductive dissolution and transformation of ferrihydrite. Environ. Sci. Tech. 53, 8736–8746.

Asta, M.P., Cama, J., Martínez, M., Giménez, J., 2009. Arsenic removal by goethite and jarosite in acidic conditions and its environmental implications. J. Hazard. Mater. 171, 965–972.

Bauer, M., Blodau, C., 2006. Mobilization of arsenic by dissolved organic matter from iron oxides, soils and sediments. Sci. Total Environ. 73, 529–542.

Bednar, A.J., Garbarino, J.R., Ranville, J.F., Wildeman, T.R., 2002. Preserving the distribution of inorganic arsenic species in groundwater and acid mine drainage samples. Environ. Sci. Tech. 36, 2213–2218.

Beesley, L., Inneh, O.S., Norton, G.J., Moreno-Jimenez, E., Pardo, T., Clemente, R., Dawson, J.J.C., 2014. Assessing the influence of compost and biochar amendments on the mobility and toxicity of metals and arsenic in a naturally contaminated mine soil. Environ. Pollut. 186, 195–202.

Bigham, J.M., Schwertmann, U., Pfab, G., 1996. Influence of pH on mineral speciation in a bioreactor simulating acid mine drainage. Appl. Geochem. 11 (583), 845–849.

Bolan, N.S., Park, J.H., Robinson, B., Naidu, R., Huh, K.Y., 2011. Phytostabilization 145–204.

Boland, D.D., Collins, R.N., Miller, C.J., Glover, C.J., Waite, T.D., 2014. Effect of solution and solid-phase conditions on the Fe(II)-accelerated transformation of ferrihydrite to lepidocrocite and goethite. Environ. Sci. Tech. 48, 5477–5485.

Bozeman, L.R., 2018. The Role of Dissolved organic matter on the mobilization of arsenic from a legacy mine tailings site. Master thesis, The University of Arizona. https://repository.arizona.edu/handle/10150/626764.

Campbell, K.M., Malsarn, D., Sltikov, C.W., Newman, D.K., Hering, J.G., 2006. Simultaneous microbial reduction of iron(III) and arsenic(V) in suspensions of hydrous ferric oxide. Environ. Sci. Tech. 40, 5950–5955.

Chen, C.M., Kukkadapu, R., Sparks, D.L., 2015. Influence of coprecipitated organic matter on $Fe^{2+}_{(aq)}$-catalyzed transformation of ferrihydrite: Implications for carbon dynamics. Environ. Sci. Tech. 49, 10927–10936.

Dixit, S., Hering, J.G., 2003. Comparison of arsenic(V) and arsenic(III) sorption onto iron oxide minerals: Implications for arsenic mobility. Environ. Sci. Tech. 37, 4182–4189.

Duquesne, K., Lieutaud, A., Ratouchniak, J., Muller, D., Lett, M.C., Bonnefoy, V., 2008. Arsenite oxidation by a chemoautotrophic moderately acidophilic Thiomonas sp.: from the strain isolation to the gene study. Environ. Microbiol. 10, 228–237.

Evangelou, V.P.B., Zhang, Y.L., 1995. A review: Pyrite oxidation mechanisms and acid mine drainage prevention. Crit. Rev. Environ. Sci. Technol. 25, 141–199.

Evanko, C.R., Dzombak, D.A., 1999. Surface complexation modeling of organic acid sorption to goethite. J. Colloid Interface Sci. 214 (2), 189–206.

Fagnano, M., Adamo, P., Zampella, M., Fiorentino, N., 2011. Environmental and agronomic impact of fertilization with composted organic fraction from municipal solid waste: a case study in the region of Naples, Italy. Agric. Ecosyst. Environ. 141, 100–107.

Fendorf, S., Kocar, B.D., 2009. Chapter 3 Biogeochemical Processes Controlling the Fate and Transport of Arsenic, pp. 137–164.

Gil-Loaiza, J., White, S.A., Root, R.A., Solís-Dominguez, F.A., Hammond, C.M., Chorover, J., Maier, R.M., 2016. Phytostabilization of mine tailings using compost-assisted direct planting: Translating greenhouse results to the field. Sci. Total Environ. 565, 451–461.

Gil-Loaiza, J., Field, J.P., White, S.A., Csavina, J., Felix, O., Betterton, E.A., Saez, A.E., Maier, R.M., 2018. Phytoremediation reduces dust emissions from metal(loid)-contaminated mine tailings. Environ. Sci. Tech. 52, 5851–5858.

Goh, K.H., Lim, T.T., 2005. Arsenic fractionation in a fine soil fraction and influence of various anions on its mobility in the subsurface environment. Appl. Geochem. 20, 229–239.

Hammond, C.M., Root, R.A., Maier, R.M., Chorover, J., 2020. Arsenic and iron speciation and mobilization during phytostabilization of pyritic mine tailings. Geochim. Cosmochim. Acta 286, 306–323.

Hansel, C.M., Benner, S.G., Neiss, J., Dohnalkova, A., Kukkadapu, R.K., Fendorf, S., 2003. Secondary mineralization pathways induced by dissimilatory iron reduction of ferrihydrite under advective flow. Geochim. Cosmochim. Acta 67, 2977–2992.

Hartley, W., Dickinson, N.M., Riby, P., Leese, E., Morton, J., Lepp, N.W., 2010. Arsenic mobility and speciation in a contaminated urban soil are affected by different methods of green waste compost application. Environ. Pollut. 158, 3560–3570.

Hayes, S.M., Root, R.A., Perdrial, N., Maier, R., Chorover, J., 2014. Surficial weathering of iron sulfide mine tailings under semiarid climate. Geochim. Cosmochim. Acta 141, 240–257.

Huang, M., Zhu, Y., Li, Z., Huang, B., Luo, N., Liu, C., Zeng, G., 2016. Compost as a soil amendment to remediate heavy metal-contaminated agricultural soil: mechanisms, efficacy, problems, and strategies. Water Air Soil Pollut. 227, 359.

Hudson-Edwards, K.A., Jamieson, H.E., Lottermoser, B.G., 2011. Mine wastes: Past, present, future. Elements 7, 375–380.

Hug, S.J., Leupin, O., 2003. Iron-catalyzed oxidation of arsenic(III) by oxygen and by hydrogen peroxide: pH-dependent formation of oxidants in the Fento reaction. Environ. Sci. Tech. 37, 2734–2742.

Islam, F.S., Gault, A.G., Boothman, C., Polya, D.A., Charnock, J.M., Chatterjee, D., Lloyd, J.R., 2004. Role of metal-reducing bacteria in arsenic release from Bengal delta sediments. Nature 430, 68–71.

Jamieson, H.E., Walker, S.R., Parsons, M.B., 2015. Mineralogical characterization of mine waste. Appl. Geochem. 57, 85–105.

Jiang, S., Lee, J.H., Kim, D., Kanaly, R.A., Kim, M.G., Hur, H.G., 2013. Differential arsenic mobilization from As-bearing ferrihydrite by iron-respiring Shewanella strains with different arsenic-reducing activities. Environ. Sci. Tech. 47, 8616–8623.

Karimian, N., Johnston, S.G., Burton, E.D., 2017. Antimony and arsenic behavior during Fe(II)-induced transformation of jarosite. Environ. Sci. Tech. 51, 4259–4268.

Kohler, J., Caravaca, F., Azcon, R., Diaz, G., Roldan, A., 2015. The combination of compost addition and arbuscular mycorrhizal inoculation produced positive and synergistic effects on the phytomanagement of a semiarid mine tailing. Sci. Total Environ. 514, 42–48.

Koschorreck, M., 2008. Microbial sulphate reduction at a low pH. FEMS Microbiol. Ecol. 64, 329–342.

Lengke, M.F., Sanpawanitchakit, C., Tempel, R.N., 2009. The oxidation and dissolution of arsenic-bearing sulfides. Can. Mineral. 47, 593–613.

Lindsay, M.B.J., Moncur, M.C., Bain, J.G., Jambor, J.L., Ptacek, C.J., Blowes, D.W., 2015. Geochemical and mineralogical aspects of sulfide mine tailings. Appl. Geochem. 57, 157–177.

Lovley, D.R., 1991. Dissimilatory Fe (III) and Mn (IV) reduction. Microbiol. Rev. 55, 259–287.

Lu, X., Wang, H., 2012. Microbial oxidation of sulfide tailings and the environmental consequences. Elements 8, 119–124.

Mendez, M.O., Glenn, E.P., Maier, R.M., 2007. Phytostabilization potential of quailbush for mine tailings. J. Environ. Qual. 36, 245–253.

Mendez, M.O., Maier, R.M., 2008. Phytostabilization of mine tailings in arid and semiarid environments – An emerging remediation technology. Environ. Health Perspect. 116, 278–283.

Mladenov, N., Zheng, Y., Simone, B., Bilinski, T.M., McKnight, D.M., Nemergut, D., Radloff, K.A., Rahman, M.M., Ahmed, K.M., 2015. Dissolved organic matter quality in a shallow aquifer of Bangladesh: Implications for arsenic mobility. Environ. Sci. Tech. 49, 10815–10824.

Nelson, K.N., Neilson, J.W., Root, R.A., Chorover, J., Maier, R.M., 2015. Abundance and activity of 16S rRNA, AmoA and NifH bacterial genes during assisted phytostabilization of mine tailings. Int. J. Phytorem. 17, 493–502.

Nordstrom, D.K., 2011. Mine waters: Acidic to circumneutral. Elements 7 (6), 393–398.

O'Day, P., 2006. Chemistry and mineralogy of arsenic. Elements 2 (2), 77–83.

Panias, D., Taxiarchou, M., Paspaliaris, I., Kontopoulos, A., 1996. Mechanisms of dissolution of iron oxides in aqueous oxalic acid solutions. Hydrometallurgy 42, 257–265.

Parsons, C.T., Couture, R.M., Omoregie, E.O., Bardelli, F., Greneche, J.M., Roman-Ross, G., Charlet, L., 2013. The impact of oscillating redox conditions: arsenic immobilization in contaminated calcareous floodplain soils. Environ. Pollut. 178, 254–263.

Phan, V.T.H., Bardelli, F., Le Pape, P., Couture, R.-M., Fernandez-Martinez, A., Tisserand, D., Bernier-Latmani, R., Charlet, L., 2018. Interplay of S and As in Mekong delta sediments during redox oscillations. Geosci. Front.

Phan, V.T.H., Bernier-Latmani, R., Tisserand, D., Bardelli, F., Le Pape, P., Frutschi, M., Gehin, A., Couture, R.M., Charlet, L., 2019. As release under the microbial sulfate reduction during redox oscillations in the upper Mekong delta aquifers, Vietnam: A mechanistic study. Sci. Total Environ. 663, 718–730.

Qiao, J., Li, X., Li, F., Liu, T., Young, L.Y., Huang, W., Sun, K., Tong, H., Hu, M., 2019. Humic substances facilitate arsenic reduction and release in flooded paddy soil. Environ. Sci. Tech. 53, 5034–5042.

Ravel, B., Newville, M., 2005. Data analysis for X-ray absorption spectroscopy using IFEFFIT. J. Synchrotron Radat. 12, 537–541.

Roberts, L.C., Hug, S.J., Ruettimann, T., Billah, M.M., Khan, A.W., Rahman, M.T., 2004. Arsenic removal with iron(II) and iron(III) in waters with high silicate and phosphate concentrations. Environ. Sci. Tech. 38, 307–315.

Root, R.A., Chorover, J., 2022. Molecular speciaiton controls arsenic and lead bioaccessibility in fugitive dusts from sulfidic mine tailings. Environ. Sci.: Process. Impacts.

Root, R.A., Vlassopoulos, D., Rivera, N.A., Rafferty, M.T., Andrews, C., O'Day, P.A., 2009. Speciation and natural attenuation of arsenic and iron in a tidally influenced shallow aquifer. Geochim. Cosmochim. Acta 73 (19), 5528–5553.

Root, R.A., Hayes, S.M., Hammond, C.M., Maier, R.M., Chorover, J., 2015. Toxic metal (loid) speciation during weathering of iron sulfide mine tailings under semiarid climate. Appl. Geochem. 62, 131–149.
Saltikov, C.W., Wildman, R., Newman, D.K., 2005. Expression dynamics of arsenic respiration and detoxification in Shewanella sp. strain ANA-3. J. Bacteriol. 187, 7390–7395.
Schippers, A., Breuker, A., Blazejak, A., Bosecker, K., Kock, D., Wright, T.L., 2010. The biogeochemistry and microbiology of sulfidic mine waste and bioleaching dumps and heaps, and novel Fe(II)-oxidizing bacteria. Hydrometallurgy 104, 342–350.
Solís-Dominguez, F.A., White, S.A., Hutter, T.B., Amistadi, M.K., Root, R.A., Chorover, J., Maier, R.M., 2012. Response of key soil parameters during compost-assisted phytostabilization in extremely acidic tailings: Effect of plant species. Environ. Sci. Tech. 46, 1019–1027.
Stookey, L., 1970. Ferrozine: A new spectrophotometric reagent for iron. Anal. Chem. 42, 779–781.
Stovern, M., Felix, O., Csavina, J., Rine, K.P., Russell, M.R., Jones, R.M., King, M., Betterton, E.A., Saez, A.E., 2014. Simulation of windblown dust transport from a mine tailings impoundment using a computational fluid dynamics model. Aeolian Res. 14, 75–83.
Thompson, A., Chadwick, O.A., Rancourt, D.G., Chorover, J., 2006. Iron-oxide crystallinity increases during soil redox oscillations. Geochim. Cosmochim. Acta 70, 1710–1727.
Valentín-Vargas, A., Root, R.A., Neilson, J.W., Chorover, J., Maier, R.M., 2014. Environmental factors influencing the structural dynamics of soil microbial communities during assisted phytostabilization of acid-generating mine tailings: a mesocosm experiment. Sci. Total Environ. 500–501, 314–324.
Valentín-Vargas, A., Neilson, J.W., Root, R.A., Chorover, J., Maier, R.M., 2018. Treatment impacts on temporal microbial community dynamics during phytostabilization of acid-generating mine tailings in semiarid regions. Sci. Total Environ. 618, 357–368.
Visconti, D., Alvarez-Robles, M.J., Fiorentino, N., Fagnano, M., Clemente, R., 2020. Use of Brassica juncea and Dactylis glomerata for the phytostabilization of mine soils amended with compost or biochar. Chemosphere 260, 127661.
Wang, S., Mulligan, C.N., 2009a. Effect of natural organic matter on arsenic mobilization from mine tailings. J. Hazard. Mater. 168, 721–726.
Wang, S., Mulligan, C.N., 2009b. Enhanced mobilization of arsenic and heavy metals from mine tailings by humic acid. Chemosphere 74, 274–279.
Webb, S., 2005. SIXPack: a graphical user interface for XAS analysis using IFEFFIT. Phys. Scr. T115, 1011.
Wiederhold, J.G., Kraemer, S.M., Teutsch, N., Borer, P.M., Halliday, A.N., Kretzschmar, R., 2006. Iron isotope fractionation during proton-promoted, ligand-controlled, and reductive dissolution of goethite. Environ. Sci. Tech. 40 (12), 3787–3793.
Winkler, P., Kaiser, K., Thompson, A., Kalbitz, K., Fiedler, S., Jahn, R., 2018. Contrasting evolution of iron phase composition in soils exposed to redox fluctuations. Geochim. Cosmochim. Acta 235, 89–102.
Ziegler, S., Dolch, K., Geiger, K., Krause, S., Asskamp, M., Eusterhues, K., Kriews, M., Wilhelms-Dick, D., Goettlicher, J., Majzlan, J., Gescher, J., 2013. Oxygen-dependent niche formation of a pyrite-dependent acidophiliv consortium built by archaea and bacteria. The ISME J. 7, 1725–1737.
Zobrist, J., Dowdle, P.R., Davis, J.A., Oremland, R.S., 2000. Mobilization of arsenite by dissimilatory reduction of adsorbed arsenate. Environ. Sci. Tech. 34, 4747–4753.